

Snow Crystal and Ice Nuclei Concentrations in Orographic Snowfall

By
Edward E. Hindman II

Department of Atmospheric Science
Colorado State University
Fort Collins, Colorado

Prepared with support from the National Science Foundation
Grant No. GP-4750
Principal investigator, Lewis O. Grant
June, 1967



**Department of
Atmospheric Science**

Paper No. 109

SNOW CRYSTAL AND ICE NUCLEI
CONCENTRATIONS IN OROGRAPHIC SNOWFALL

by
Edward E. Hindman II

This report was prepared with support from
the National Science Foundation
Grant No. GP-4750
Principal Investigator, Lewis O. Grant

Department of Atmospheric Science
Colorado State University
Fort Collins, Colorado

June 1967

Atmospheric Science Paper No. 109

ABSTRACT

Concentrations of snow crystals and ice nuclei within orographic cloud systems have not as yet been simultaneously monitored. Ground observations of these parameters however have been simultaneously obtained near Climax in the Central Colorado Rockies. The objective of this report is to determine the relationship between snow crystal and ice nuclei concentrations for similar crystal formation and nuclei activation temperatures. In this investigation, it is assumed that the ice nuclei and snow crystal concentrations measured in a volume of air at the ground can be used to represent the ice nuclei and snow crystal concentrations in a similar volume of air in the cloud. A continuous snowfall replicator is described which measures the necessary snow crystal concentrations.

In the two unseeded orographic snowfall periods investigated, the average snow crystal and ice nuclei concentrations measured at the ground were approximately equal for the same crystal formation and nuclei activation temperatures. This determination considers an adjustment of the nuclei concentration by an average factor of 3.5 in the Bigg-Warner expansion-type ice nuclei counter. This factor is an average of the values presented by Warner and Newnham (1958) and Fletcher (1958).

In the two seeded orographic snowfall periods, the average ice nuclei concentrations at the ground were larger than the snow crystal concentrations by at least an order of magnitude. If the ground-released artificial ice nuclei plume is assumed only partially dispersed and activated in the cloud and almost totally activated in the Bigg-Warner counter, this would explain the larger nuclei concentrations. The ice nuclei concentrations at the ground in these two seeded snowfall periods might not represent the in-cloud nuclei concentrations.

These snow crystal and ice nuclei relationships in unseeded and seeded snowfall were not firmly established because of a limited sample and a lack of a priori information. The techniques and procedures developed in this thesis should form the basis for the analysis of more elaborate data collected subsequent to the preparation of this manuscript.

Edward E. Hindman, II
Atmospheric Science Department
Colorado State University
June 1967

ACKNOWLEDGMENTS

The author wishes to express his appreciation to Professor Lewis O. Grant for his guidance during the two years this study was in progress. He especially wishes to thank his fiancée, Nancy Maxson, for editing and typing the manuscript. He is also grateful to William Ehrman and Allen Eddy for developing the snow crystal computer program, and to Timothy Smith and Daniel Rudolph for reducing the snow crystal replica data. Lilah Roberts is recognized for a fine printing job under a strict time schedule. The National Center for Atmospheric Research is acknowledged for use of their computer.

This research was sponsored by the National Science Foundation under Contract GP 4750.

This material is based upon a thesis submitted as partial fulfillment of the requirements for the Master of Science Degree at Colorado State University.

TABLE OF CONTENTS

	Page
TITLE PAGE	i
ABSTRACT	ii
ACKNOWLEDGMENTS	iv
LIST OF TABLES	vii
LIST OF FIGURES	viii
INTRODUCTION	1
Background	1
Objectives	3
THEORY	4
Ice Nuclei Concentrations	4
Snow Crystal Concentrations	7
PROCEDURE	10
Experimental Design	10
Instrumentation	14
Ice Nuclei Counter	14
Continuous Snowfall Replicator	15
DATA AND ANALYSIS	27
Unseeded Orographic Snowfall	27
Seeded Orographic Snowfall	33
DISCUSSION	38
Unseeded Orographic Snowfall	38
Seeded Orographic Snowfall	42
Total Nuclei and Crystal Concentrations	46
SUMMARY AND CONCLUSIONS	50
Snow Crystal and Ice Nuclei Concentrations	50
Instrumentation	52

TABLE OF CONTENTS - Continued

	Page
RECOMMENDATIONS	53
REFERENCES	54
APPENDICES	59
APPENDIX A. THE CONTINUOUS SNOWFALL REPLICATOR SYSTEM	60
Operation of the Continuous Snowfall Replicator	60
Data Reduction System	61
Snow Crystal Concentration Program	69
APPENDIX B. TERMINAL VELOCITIES OF SNOW CRYSTALS .	77

LIST OF FIGURES

Figure		Page
1	Location of Climax, Colorado	2
2	Snow crystal formation temperatures, W = saturation with respect to supercooled water [from Nakaya (1954)]	9
3	Schematic diagram of a simplified orographic cloud. . .	11
4	Continuous snowfall replicator	17
5	Formvar reservoir and "roll on" coating wheel	17
6	Snow crystal sampling slit and 35 mm film transport passed the coating wheel	18
7	Typical snow crystal replicas from the continuous snowfall replicator	18
8	Typical snow crystal concentration computation, HAO, Climax, Colorado, 5 January 1967 (Original data in Table 7)	20
9	Typical snow crystal concentrations plotted against time, HAO, Climax, Colorado, 5 January 1967	23
10	Comparison of total snow crystal concentrations observed by three simultaneously-operating replicators, Climax, Colorado, 27 December 1966	26
11	Snow crystal concentrations, HAO, Climax, Colorado, 8 February 1966	31
12	Snow crystal concentrations, HAO, Climax, Colorado, 11 April 1966	36
13	Schematic diagram of the unseeded orographic cloud system, Climax, Colorado, 8 February 1966, 0630 to 1215 MST	39
14	Schematic diagram of the seeded orographic cloud system, Climax, Colorado, 11 April 1966, 1600 to 1800 MST	43
15	The snow crystal replica film-strip projector	62
16	Snow crystal dimension scale (full size)	63
17	General classification of snow crystals, sketches [from Nakaya (1954)]	65

LIST OF FIGURES - Continued

Figure		Page
18	Snow crystal concentration computer program flow-chart	71
19	Snow crystal concentration computer program	73
20	Terminal velocities of various snow crystals [from Todd (1964)]	78

INTRODUCTION

Background

Supercooled orographic cloud systems should be susceptible to artificial stimulation of snowfall according to Bergeron (1949). Supercooled water may not be utilized because of a natural deficiency of ice nuclei (Ludlam, 1955). Bergeron (1949) states that the supercooled water, which may not precipitate under natural conditions, may precipitate by introducing artificial ice nuclei into clouds upwind of orographic barriers.

An orographic cloud seeding experiment is being conducted by the Atmospheric Science Department of Colorado State University in the Central Colorado Rockies in the vicinity of Climax. The location of Climax is illustrated in Figure 1. This experiment is designed to investigate supercooled orographic cloud systems in a systematic manner. The first step is to study the concentrations and nucleating characteristics of natural and artificial ice nuclei. This objective is progressing well as a result of work by Grant and Schleusener (1961) and Grant and Steele (1966). The second step is an investigation of the transport of nuclei into the cloud system. The transport of ground-released ice nuclei to the mountain top is becoming well established. The study of further transport within the cloud presents numerous problems but is progressing. The third step is designed to improve the

LIST OF TABLES

Table		Page
1	Snow crystal and ice nuclei concentrations, HAO, Climax, Colorado, 8 February 1966 (number/liter) . . .	29
2	Contingency tables for the 8 February 1966 snow crystal and ice nuclei concentrations	32
3	Snow crystal and ice nuclei concentrations, HAO, Climax, Colorado, 11 April 1966 (number/liter)	35
4	Total snow crystal and ice nuclei concentrations	48
5	General classification of snow crystals [from Nakaya (1954)]	66
6	Numerical snow crystal types [after Nakaya (1954)]	67
7	Typical snow crystal replica data, HAO, Climax, Colorado, 5 January 1967	68
8	Hexagonal plate terminal velocity equation and solutions	80
9	Needle terminal velocity equation and solutions (crystal dimension ≤ 0.010 cm)	82
10	Needle terminal velocity equation and solutions (crystal dimension ≥ 0.011 cm)	83



Figure 1. Location of Climax, Colorado

understanding of in-cloud physical processes. A first look at these processes may be obtained from snow crystal and ice nuclei concentrations measured at the ground. The relationship between these concentrations will be treated in this report. The final step is to statistically analyze precipitation amounts from unseeded and seeded storms. Preliminary results of this analysis show that precipitation can be increased in certain supercooled cloud systems (Grant and Mielke, 1965). The primary objective of the Climax experiment is to understand each step so cloud seeding may become operationally feasible for increasing mountain snow packs.

Objectives

The main objective of this report is to establish a preliminary relationship between in-cloud snow crystal and mountain-top ice nuclei concentrations for orographic snowfall. A relationship is sought both for unseeded and for seeded snowfall. To relate the snow crystal and ice nuclei concentrations, orographic cloud systems are simplified so the volume of air in an ice nuclei counter can be compared with in-cloud conditions.

The second objective is to present in detail the snow crystal concentration calibration and analysis scheme used with the recently developed continuous snowfall replicator (Hindman and Reinking, 1966a; Hindman and Rinker, 1967). This discussion is necessary to substantiate the snow crystal concentrations discussed in this report.

THEORY

The orographic cloud seeding experiment at Climax is based on the physical concept presented by Bergeron (1949) and discussed more explicitly by Ludlam (1955). This concept envisages artificial ice nuclei being released from the ground, far enough upwind of the orographic barrier so the snow crystals produced by these and natural nuclei will grow in saturated conditions with respect to supercooled water. These conditions will exist only if excessive concentrations of crystals are not present. Ludlam (1955) has computed that the optimum concentration of snow crystals is 20 per liter. Crystals growing with this concentration should be large enough to fall from the cloud before the air descends and warms, thus dissipating the cloud on the downwind side of the barrier. The ice nuclei concentration in an orographic cloud is an important parameter therefore for the production of snow crystals.

Ice Nuclei Concentrations

The geographic source regions for natural ice nuclei have been studied extensively in Japan by Kumai (1951) and Isono (1955). In these studies, they found the observed nuclei to consist of sub-microscopic clay particles which have their source in the interior of the Asiatic continent. Furthermore, Schaefer (1954) found that dust

particles originating in the central region of the United States contribute to the natural ice nuclei counts downwind in New Hampshire. Recently, Droessler (1965) has concluded that another possible source of ice nuclei is in the upper atmosphere. This supports Bowen's (1956) theory of an extra-terrestrial origin of ice nuclei.

The concentrations with altitude of natural ice nuclei have been measured by Smith and Heffernan (1954) over Australia and by Kassander, et al. (1957) over the Southwest United States. They have found that natural ice nuclei concentrations are nearly uniform for thin atmospheric layers (approximately 2 km) when low-level temperature inversions are absent. Orographic clouds at Climax are generally about 2 km thick. It appears reasonable to assume that natural ice nuclei concentrations are uniform in orographic clouds at Climax.

The temperatures at which the natural ice nuclei concentrations begin to form ice crystals within orographic clouds can be inferred from measurements by Schaefer (1951). His measurements were made in an artificial supercooled cloud at water-saturation in a cloud chamber, and these conditions are a reasonable facsimile to those occurring in a supercooled orographic cloud. He found that the average threshold activation temperature is approximately -12°C . The nuclei activate in greater concentrations as the temperature is reached at which the total concentration is activated (about -23°C).

Consequently, in supercooled orographic clouds with cloud tops warmer than -23°C --containing only natural ice nuclei--only a portion of the nuclei concentration capable of serving as ice nuclei at -23°C or colder will be activated.

Silver iodide (AgI) ice nuclei may be introduced into clouds with tops warmer than -23°C to increase the concentrations of active natural ice nuclei. The AgI nuclei are able to increase this concentration because the AgI nuclei threshold activation temperature at water-saturation is approximately -8°C for the CSU modified Skyfire generators used in the Climax experiment (Grant and Mielke, 1965). These nuclei activate in greater concentrations as the total activation temperature is approached (approximately -23°C).

The concentrations of ground-released AgI nuclei with altitude have been measured from aircraft observations by Smith and Heffernan (1954) and Henderson (1965). They have found that the plumes diffuse erratically and non-uniformly with altitude. These characteristics are probably a result of erratic diffusion patterns and photolytic decay of the AgI nuclei (Reynolds et al., 1951; Bryant and Mason, 1960). It appears realistic, therefore, to expect that the AgI nuclei concentration--when subjected to short mixing times--is erratic with height in an orographic cloud. Natural nuclei originate from large continental areas and have long mixing times, while the AgI nuclei originate from point sources relatively near the cloud systems. This combination

of the larger source areas and greater distance from source to cloud should enable the natural nuclei to diffuse more uniformly than the AgI nuclei. The degree of uniformity of these two nuclei concentrations may be an important factor to consider when relating snow crystal and ice nuclei concentrations.

Snow Crystal Concentrations

To relate the concentrations of snow crystals and ice nuclei, it is initially assumed that one ice crystal forms on one ice nucleus. Kepler (1611) was probably the first to discuss this concept. Kumai (1951) supports this assumption from observations with an electron microscope that indicate one solid nucleus is always found in the central portion of a snow crystal. Snow crystals do, in most cases, aggregate to form snowflakes (Hosler, et al., 1957; Hosler and Hallgren, 1961; and Hobbs, 1965). Furthermore, large snowflakes fracture and form crystal fragments which do not possess a central nucleus (Schaefer, 1951). In both these processes however the original crystal formed from a single nucleus.

To relate snow crystal and ice nuclei concentrations, it must be further assumed that the formation temperature (T_f) of a snow crystal is the same as the activation temperature (T_a) of the ice nucleus. Hindman (1966) determined, for example, that a column reaches 15μ in approximately ten seconds after activation. This

growth rate is in agreement with those presented by Fletcher (1962). The crystal for practical purposes reaches the characteristic shape before settling from the T_a level in the cloud. While falling from the T_a level, the crystal encounters different temperatures and supersaturations. These conditions may somewhat alter the crystal form. For simplicity, it is assumed in this study that the crystal attains a substantial portion of its size near the T_a level, thereby being identifiable as forming at that level when observed at the ground.

Nakaya (1954) and Magono (1962) have meticulously studied the formation of the various snow crystal types in the laboratory at different supercoolings and supersaturations. From snow crystal replicas obtained in natural clouds by Magono and Tazawa (1966) with their "snow crystal sondes," they have verified these laboratory-produced snow crystal formation temperatures in Figure 2.

It is possible to estimate the levels at which snow crystals form by using the appropriate formation temperatures for their shapes, the upper-air temperature profile, and the height of the snow-generating cloud. For example, columns form at approximately -10C and -20C. If the elevation of the -20C upper-air temperature is low enough to be in the snow-generating cloud and no portion of the cloud is warmer than -10C, it is highly probable that columns formed at the -20C level. If however the -20C isotherm is higher than the snow-generating cloud top, the columns may have formed in cirrus clouds above.

PROCEDURE

Experimental Design

A simplified description of an orographic cloud is presented in Figure 3. This description permits a comparison of the ice nuclei concentrations measured in the artificial supercooled cloud of an ice nuclei counter and the snow crystal concentrations measured from orographic snowfall. This concept is developed from the previous ice nuclei and snow crystal concentration theory.

The isotherm T_1 in Figure 3 is defined as the threshold ice nuclei activation temperature. T_1 is not necessarily at cloud base, but is assumed at the -8 and -12C levels for AgI and natural ice nuclei, respectively. T_2 is an arbitrary snow crystal formation temperature isotherm and T_3 is the cloud-top temperature.

The in-cloud snow crystal concentration which form in a column of air from T_1 to T_2 in Figure 3 is found by summing the concentrations of snow crystals at the ground with $T_1 \geq T_f \geq T_2$. When this column of air is projected from T_1 to T_3 it contains all snow crystals produced by the activation of all ice nuclei within the temperature range in the cloud. This total in-cloud snow crystal concentration is found by summing the concentrations of snow crystals at the ground with $T_1 \geq T_f \geq T_3$.

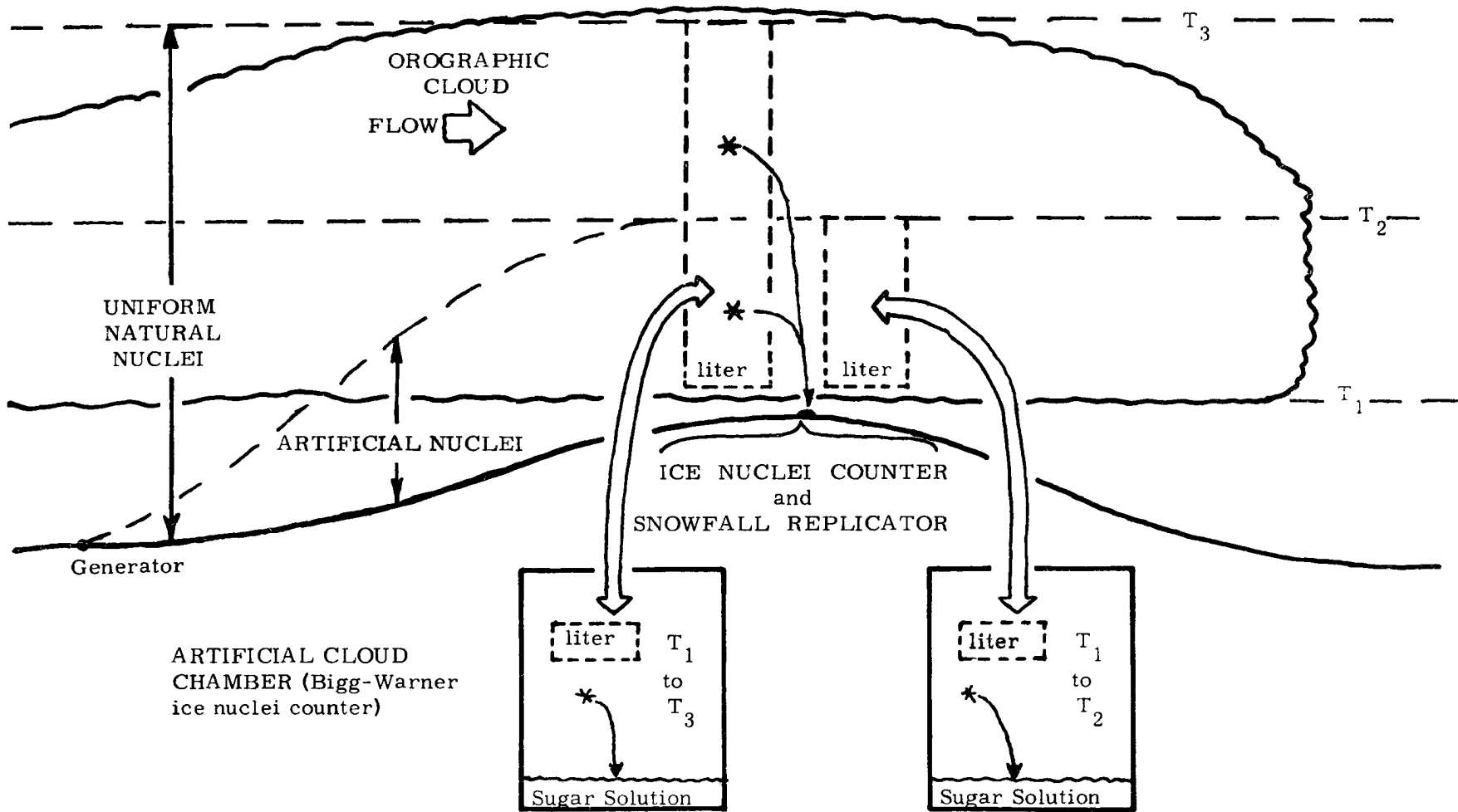


Figure 3. Schematic diagram of a simplified orographic cloud

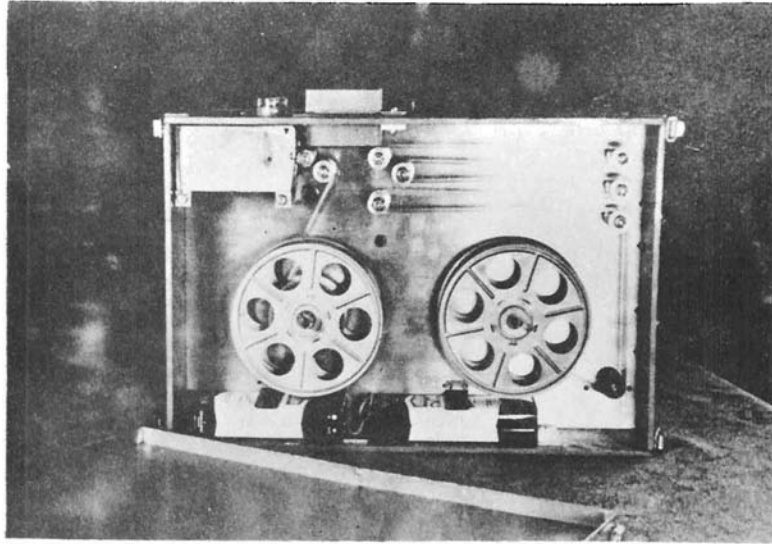


Figure 4. Continuous snowfall replicator

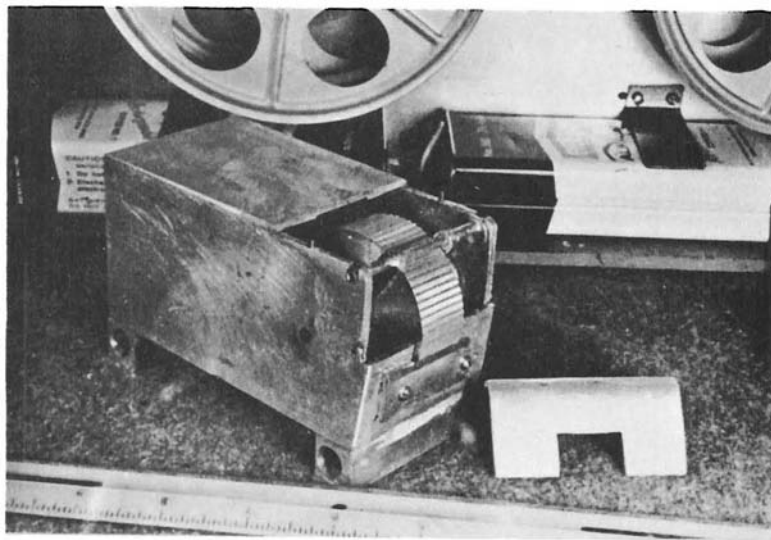


Figure 5. Formvar reservoir and "roll-on" coating wheel

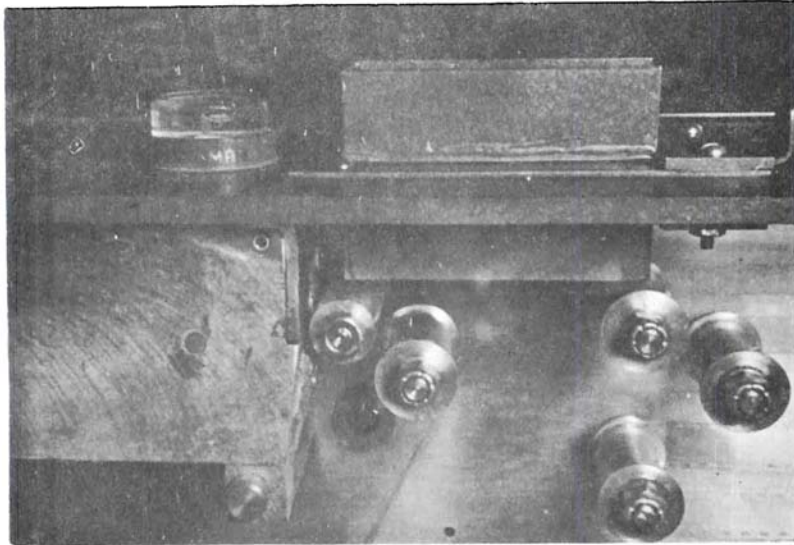
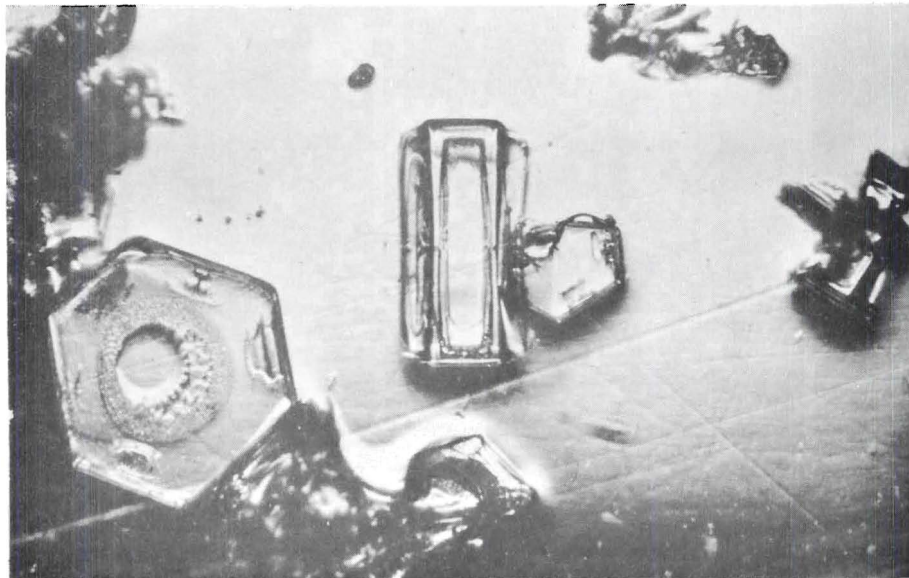


Figure 6. Snow crystal sampling slit and 35 mm film transport mechanism passed the coating wheel



500 μ

Figure 7. Typical snow crystal replicas from the continuous snowfall replicator

A (cm^2), and V is the volume (cm^3) from which the crystals settle. The crystal types are classified according to Nakaya (1954) and are illustrated in Figure 17. The terminal velocities of the different crystal types are obtained from Nakaya (1954) and Todd (1964) (see Appendix B).

The most important error associated with the calibration computation is in the determination of the V_t term. The V_t values in Appendix B are only approximate. From Nakaya's (1954) original data, it appears that the V_t scatter around the mean values varies a maximum of $\pm 15\%$. Assuming that V_t values are underestimated (overestimated) by 15%, the concentration will be overestimated (underestimated) by 15%. For example, concentrations computed as 4.0 per liter would be expected to range from 3.4 to 4.6, deviating from the computed value by a factor of ± 1.15 . This factor may be neglected because the variability of the snow crystal concentrations is greater than a factor of ± 1.15 over short time intervals as illustrated in Figure 8.

Figure 8 is a very small sample of the mass of print out received from the computer for each analyzed snowfall period. The calibration computation produces a concentration for each different size snow crystal of a particular type observed within the sampling area (4.50 cm^2) on the film. At 2124 MST, crystal type 311 with a size of 130μ had a concentration of 0.7 per liter. The total snow

SITE 1 DATE 10567

TIME 2110 TYPE 311 TERMINAL VELOCITY 25.1555 EXPOSURE TIME 18.02 LENGTH .021000 WIDTH 0
NUMBER OF CRYSTALS / LITER .4902838957 NUMBER OF CRYSTALS / CM. SQUARED SEC. .0123333333
SURFACE TEMPERATURE -9 FORMATION TEMPERATURE -14 KEQ = 1

TIME 2110 TYPE 61 TERMINAL VELOCITY 120.0000 EXPOSURE TIME 18.02 LENGTH .011000 WIDTH 0
NUMBER OF CRYSTALS / LITER .1027777778 NUMBER OF CRYSTALS / CM. SQUARED SEC. .0123333333
SURFACE TEMPERATURE -9 FORMATION TEMPERATURE -25 KEQ = 6

TIME 2110 (CMST)

SUM OF REGULAR CRYSTALS PER LITER .4902838957
SUM OF IRREGULAR CRYSTALS PER LITER .1027777778
SUM OF RIME CRYSTALS PER LITER 0.
SUM OF TOTAL CRYSTALS PER LITER .5930616735

CONCENTRATION OF CRYSTALS
AT FORMATION TEMPERATURE GREATER THAN OR EQUAL TO -14 .49028
AT FORMATION TEMPERATURE GREATER THAN OR EQUAL TO -20 .49028
AT FORMATION TEMPERATURE GREATER THAN OR EQUAL TO -26 .59306

TIME 2112 TYPE 311 TERMINAL VELOCITY 14.7675 EXPOSURE TIME 18.02 LENGTH .011000 WIDTH 0
NUMBER OF CRYSTALS / LITER .8351664214 NUMBER OF CRYSTALS / CM. SQUARED SEC. .0123333333
SURFACE TEMPERATURE -9 FORMATION TEMPERATURE -14 KEQ = 1

TIME 2112 TYPE 219 TERMINAL VELOCITY 96.1126 EXPOSURE TIME 18.02 LENGTH .011000 WIDTH .015000
NUMBER OF CRYSTALS / LITER .1283216480 NUMBER OF CRYSTALS / CM. SQUARED SEC. .0123333333
SURFACE TEMPERATURE -9 FORMATION TEMPERATURE -20 KEQ = 4

TIME 2112 TYPE 61 TERMINAL VELOCITY 120.0000 EXPOSURE TIME 18.02 LENGTH .010000 WIDTH 0
NUMBER OF CRYSTALS / LITER .1027777778 NUMBER OF CRYSTALS / CM. SQUARED SEC. .0123333333
SURFACE TEMPERATURE -9 FORMATION TEMPERATURE -25 KEQ = 6

TIME 2112

SUM OF REGULAR CRYSTALS PER LITER .9634880694
SUM OF IRREGULAR CRYSTALS PER LITER .1027777778
SUM OF RIME CRYSTALS PER LITER 0.
SUM OF TOTAL CRYSTALS PER LITER 1.0662658472

CONCENTRATION OF CRYSTALS
AT FORMATION TEMPERATURE GREATER THAN OR EQUAL TO -14 .83517
AT FORMATION TEMPERATURE GREATER THAN OR EQUAL TO -20 .96349
AT FORMATION TEMPERATURE GREATER THAN OR EQUAL TO -26 1.06627

TIME 2124 TYPE 311 TERMINAL VELOCITY 17.2332 EXPOSURE TIME 18.02 LENGTH .013000 WIDTH 0
NUMBER OF CRYSTALS / LITER .7156739889 NUMBER OF CRYSTALS / CM. SQUARED SEC. .0123333333
SURFACE TEMPERATURE -9 FORMATION TEMPERATURE -14 KEQ = 1

TIME 2124 TYPE 311 TERMINAL VELOCITY 25.1555 EXPOSURE TIME 18.02 LENGTH .021000 WIDTH 0
NUMBER OF CRYSTALS / LITER 1.9611355828 NUMBER OF CRYSTALS / CM. SQUARED SEC. .0493333333
SURFACE TEMPERATURE -9 FORMATION TEMPERATURE -14 KEQ = 1

TIME 2124 TYPE 311 TERMINAL VELOCITY 30.3737 EXPOSURE TIME 18.02 LENGTH .029000 WIDTH 0
NUMBER OF CRYSTALS / LITER .4060530060 NUMBER OF CRYSTALS / CM. SQUARED SEC. .0123333333
SURFACE TEMPERATURE -9 FORMATION TEMPERATURE -14 KEQ = 1

TIME 2124 TYPE 212 TERMINAL VELOCITY 58.1800 EXPOSURE TIME 18.02 LENGTH .021000 WIDTH .009000
NUMBER OF CRYSTALS / LITER .2119859315 NUMBER OF CRYSTALS / CM. SQUARED SEC. .0123333333
SURFACE TEMPERATURE -9 FORMATION TEMPERATURE -20 KEQ = 3

TIME 2124 TYPE 213 TERMINAL VELOCITY 22.3219 EXPOSURE TIME 18.02 LENGTH .017000 WIDTH .004000
NUMBER OF CRYSTALS / LITER .5525228725 NUMBER OF CRYSTALS / CM. SQUARED SEC. .0123333333
SURFACE TEMPERATURE -9 FORMATION TEMPERATURE -20 KEQ = 3

TIME 2124 TYPE 213 TERMINAL VELOCITY 22.3219 EXPOSURE TIME 18.02 LENGTH .019000 WIDTH .004000
NUMBER OF CRYSTALS / LITER .5525228725 NUMBER OF CRYSTALS / CM. SQUARED SEC. .0123333333
SURFACE TEMPERATURE -9 FORMATION TEMPERATURE -20 KEQ = 3

TIME 2124 TYPE 213 TERMINAL VELOCITY 58.1800 EXPOSURE TIME 18.02 LENGTH .015000 WIDTH .009000
NUMBER OF CRYSTALS / LITER .2119859315 NUMBER OF CRYSTALS / CM. SQUARED SEC. .0123333333
SURFACE TEMPERATURE -9 FORMATION TEMPERATURE -20 KEQ = 3

TIME 2124 TYPE 219 TERMINAL VELOCITY 58.1800 EXPOSURE TIME 18.02 LENGTH .021000 WIDTH .009000
NUMBER OF CRYSTALS / LITER .4239718631 NUMBER OF CRYSTALS / CM. SQUARED SEC. .0246666667
SURFACE TEMPERATURE -9 FORMATION TEMPERATURE -20 KEQ = 3

TIME 2124 TYPE 213 TERMINAL VELOCITY 71.4044 EXPOSURE TIME 18.02 LENGTH .021000 WIDTH .011000
NUMBER OF CRYSTALS / LITER .3454503892 NUMBER OF CRYSTALS / CM. SQUARED SEC. .0246666667
SURFACE TEMPERATURE -9 FORMATION TEMPERATURE -20 KEQ = 4

TIME 2124 TYPE 213 TERMINAL VELOCITY 96.1126 EXPOSURE TIME 18.02 LENGTH .021000 WIDTH .015000
NUMBER OF CRYSTALS / LITER .1283216480 NUMBER OF CRYSTALS / CM. SQUARED SEC. .0123333333
SURFACE TEMPERATURE -9 FORMATION TEMPERATURE -20 KEQ = 4

TIME 2124 TYPE 222 TERMINAL VELOCITY 233.5991 EXPOSURE TIME 18.02 LENGTH .045000 WIDTH .013000
NUMBER OF CRYSTALS / LITER .0527970041 NUMBER OF CRYSTALS / CM. SQUARED SEC. .0123333333
SURFACE TEMPERATURE -9 FORMATION TEMPERATURE -20 KEQ = 4

TIME 2124 TYPE 43 TERMINAL VELOCITY 120.0000 EXPOSURE TIME 18.02 LENGTH .025000 WIDTH 0
NUMBER OF CRYSTALS / LITER .5138888889 NUMBER OF CRYSTALS / CM. SQUARED SEC. .0616666667
SURFACE TEMPERATURE -9 FORMATION TEMPERATURE -25 KEQ = 6

Figure 8. Typical snow crystal concentration computation, HAO, Climax, Colorado, 5 January 1967. (Original data in Table 7)

Figure 8. Continued

```

TIME 2124 TYPE 610 TERMINAL VELOCITY 89.2674 EXPOSURE TIME 18.02 LENGTH .017000 WIDTH 0
NUMBER OF CRYSTALS / LITER .1381616408 NUMBER OF CRYSTALS / CM. SQUARED SEC. .0123333333
SURFACE TEMPERATURE -9 FORMATION TEMPERATURE -25 KEQ = 5

TIME 2124 TYPE 61 TERMINAL VELOCITY 120.0000 EXPOSURE TIME 18.02 LENGTH .011000 WIDTH 0
NUMBER OF CRYSTALS / LITER 4.9333333333 NUMBER OF CRYSTALS / CM. SQUARED SEC. .5920000000
SURFACE TEMPERATURE -9 FORMATION TEMPERATURE -25 KEQ = 6

TIME 2124 (MST)
SUM OF REGULAR CRYSTALS PER LITER 5.5624210901
SUM OF IRREGULAR CRYSTALS PER LITER 5.4472222222
SUM OF RIME CRYSTALS PER LITER .1381616408
SUM OF TOTAL CRYSTALS PER LITER 11.1478049531

CONCENTRATION OF CRYSTALS
AT FORMATION TEMPERATURE GREATER THAN OR EQUAL TO -14 3.08286
AT FORMATION TEMPERATURE GREATER THAN OR EQUAL TO -20 5.56242
AT FORMATION TEMPERATURE GREATER THAN OR EQUAL TO -26 11.14780

```

(2125 to 2359 and a portion of 2400 MST deleted)

```

TIME 2400 TYPE 213 TERMINAL VELOCITY 15.7353 EXPOSURE TIME 9.52 LENGTH .025000 WIDTH .003000
NUMBER OF CRYSTALS / LITER 3.0430954069 NUMBER OF CRYSTALS / CM. SQUARED SEC. .0466666667
SURFACE TEMPERATURE -12 FORMATION TEMPERATURE -20 KEQ = 3

TIME 2400 TYPE 213 TERMINAL VELOCITY 145.5795 EXPOSURE TIME 9.52 LENGTH .025000 WIDTH .024000
NUMBER OF CRYSTALS / LITER .1602790051 NUMBER OF CRYSTALS / CM. SQUARED SEC. .0233333333
SURFACE TEMPERATURE -12 FORMATION TEMPERATURE -20 KEQ = 4

TIME 2400 TYPE 213 TERMINAL VELOCITY 15.7353 EXPOSURE TIME 9.52 LENGTH .028000 WIDTH .003000
NUMBER OF CRYSTALS / LITER 1.5215479034 NUMBER OF CRYSTALS / CM. SQUARED SEC. .0233333333
SURFACE TEMPERATURE -12 FORMATION TEMPERATURE -20 KEQ = 3

TIME 2400 TYPE 213 TERMINAL VELOCITY 15.7353 EXPOSURE TIME 9.52 LENGTH .031000 WIDTH .003000
NUMBER OF CRYSTALS / LITER 1.5215479034 NUMBER OF CRYSTALS / CM. SQUARED SEC. .0233333333
SURFACE TEMPERATURE -12 FORMATION TEMPERATURE -20 KEQ = 3

TIME 2400 TYPE 213 TERMINAL VELOCITY 29.5303 EXPOSURE TIME 9.52 LENGTH .033000 WIDTH .005000
NUMBER OF CRYSTALS / LITER .7901476338 NUMBER OF CRYSTALS / CM. SQUARED SEC. .0233333333
SURFACE TEMPERATURE -12 FORMATION TEMPERATURE -20 KEQ = 3

TIME 2400 TYPE 222 TERMINAL VELOCITY 107.8165 EXPOSURE TIME 9.52 LENGTH .017000 WIDTH .014000
NUMBER OF CRYSTALS / LITER .2164171203 NUMBER OF CRYSTALS / CM. SQUARED SEC. .0233333333
SURFACE TEMPERATURE -12 FORMATION TEMPERATURE -20 KEQ = 4

TIME 2400 TYPE 430 TERMINAL VELOCITY 88.3338 EXPOSURE TIME 9.52 LENGTH .015000 WIDTH 0
NUMBER OF CRYSTALS / LITER .2641495297 NUMBER OF CRYSTALS / CM. SQUARED SEC. .0233333333
SURFACE TEMPERATURE -12 FORMATION TEMPERATURE -25 KEQ = 5

TIME 2400 TYPE 430 TERMINAL VELOCITY 89.2674 EXPOSURE TIME 9.52 LENGTH .017000 WIDTH 0
NUMBER OF CRYSTALS / LITER .2613868880 NUMBER OF CRYSTALS / CM. SQUARED SEC. .0233333333
SURFACE TEMPERATURE -12 FORMATION TEMPERATURE -25 KEQ = 5

TIME 2400 TYPE 430 TERMINAL VELOCITY 90.1054 EXPOSURE TIME 9.52 LENGTH .019000 WIDTH 0
NUMBER OF CRYSTALS / LITER .5179122708 NUMBER OF CRYSTALS / CM. SQUARED SEC. .0466666667
SURFACE TEMPERATURE -12 FORMATION TEMPERATURE -25 KEQ = 5

TIME 2400 TYPE 430 TERMINAL VELOCITY 93.8879 EXPOSURE TIME 9.52 LENGTH .031000 WIDTH 0
NUMBER OF CRYSTALS / LITER .2485233078 NUMBER OF CRYSTALS / CM. SQUARED SEC. .0233333333
SURFACE TEMPERATURE -12 FORMATION TEMPERATURE -25 KEQ = 5

TIME 2400 TYPE 430 TERMINAL VELOCITY 99.3809 EXPOSURE TIME 9.52 LENGTH .061000 WIDTH 0
NUMBER OF CRYSTALS / LITER .2347868675 NUMBER OF CRYSTALS / CM. SQUARED SEC. .0233333333
SURFACE TEMPERATURE -12 FORMATION TEMPERATURE -25 KEQ = 5

TIME 2400 TYPE 43 TERMINAL VELOCITY 120.0000 EXPOSURE TIME 9.52 LENGTH .025000 WIDTH 0
NUMBER OF CRYSTALS / LITER 10.5000000000 NUMBER OF CRYSTALS / CM. SQUARED SEC. 1.2600000000
SURFACE TEMPERATURE -12 FORMATION TEMPERATURE -25 KEQ = 6

TIME 2400 TYPE 61 TERMINAL VELOCITY 120.0000 EXPOSURE TIME 9.52 LENGTH .023000 WIDTH 0
NUMBER OF CRYSTALS / LITER .1944444444 NUMBER OF CRYSTALS / CM. SQUARED SEC. .0233333333
SURFACE TEMPERATURE -12 FORMATION TEMPERATURE -25 KEQ = 6

TIME 2400
SUM OF REGULAR CRYSTALS PER LITER 83.6459610945
SUM OF IRREGULAR CRYSTALS PER LITER 10.6944444444
SUM OF RIME CRYSTALS PER LITER 1.5267588438
SUM OF TOTAL CRYSTALS PER LITER 95.8671644028

CONCENTRATION OF CRYSTALS
AT FORMATION TEMPERATURE GREATER THAN OR EQUAL TO -14 0.
AT FORMATION TEMPERATURE GREATER THAN OR EQUAL TO -20 83.64596
AT FORMATION TEMPERATURE GREATER THAN OR EQUAL TO -26 95.86716

AVERAGES OF CONCENTRATION OF CRYSTALS
AT FORMATION TEMPERATURE GREATER THAN OR EQUAL TO -14 .57757
AT FORMATION TEMPERATURE GREATER THAN OR EQUAL TO -20 19.73905
AT FORMATION TEMPERATURE GREATER THAN OR EQUAL TO -26 25.97386

```

crystal concentration for a time period is simply a sum of all the individual crystal concentrations (for 2124 MST, it is 11.14 per liter). The total crystal concentration is separated into categories of plane, irregular, and rimed, according to Nakaya's (1954) classification in Figure 17. The concentration in each category is found by adding the total concentrations of each crystal type in that category (for 2124 MST the concentration of regular crystals is the sum of the total concentrations of type 311, 212, 222, and 213, or 5.56 per liter). The total snow crystal concentration is also divided into formation temperature ranges: $T_f \geq -14\text{C}$; $T_f \geq -20\text{C}$; and, $T_f \geq -26\text{C}$. At the end of the snowfall period (2400 MST), the averages for the formation temperature ranges are determined. The concentrations (total, irregular, plane) are graphed against time in Figure 9. Appendix A gives the details of this analysis procedure.

The major error associated with the analysis procedure in Figure 8 is the identification of irregular snow crystals. In most cases, irregular crystals are not identified with Nakaya's classification. The unidentified irregular crystals are assumed either fragments of larger snowflakes (Schaefer, 1951) or crystals forming with irregular shapes. The fragments would not be expected to contain ice nuclei. It is difficult to estimate how much this error affects the total crystal concentration. This error however does not affect the crystal concentration with $T_f \geq -20\text{C}$ because the fragments are considered irregular crystals with $T_f \sim -25\text{C}$.

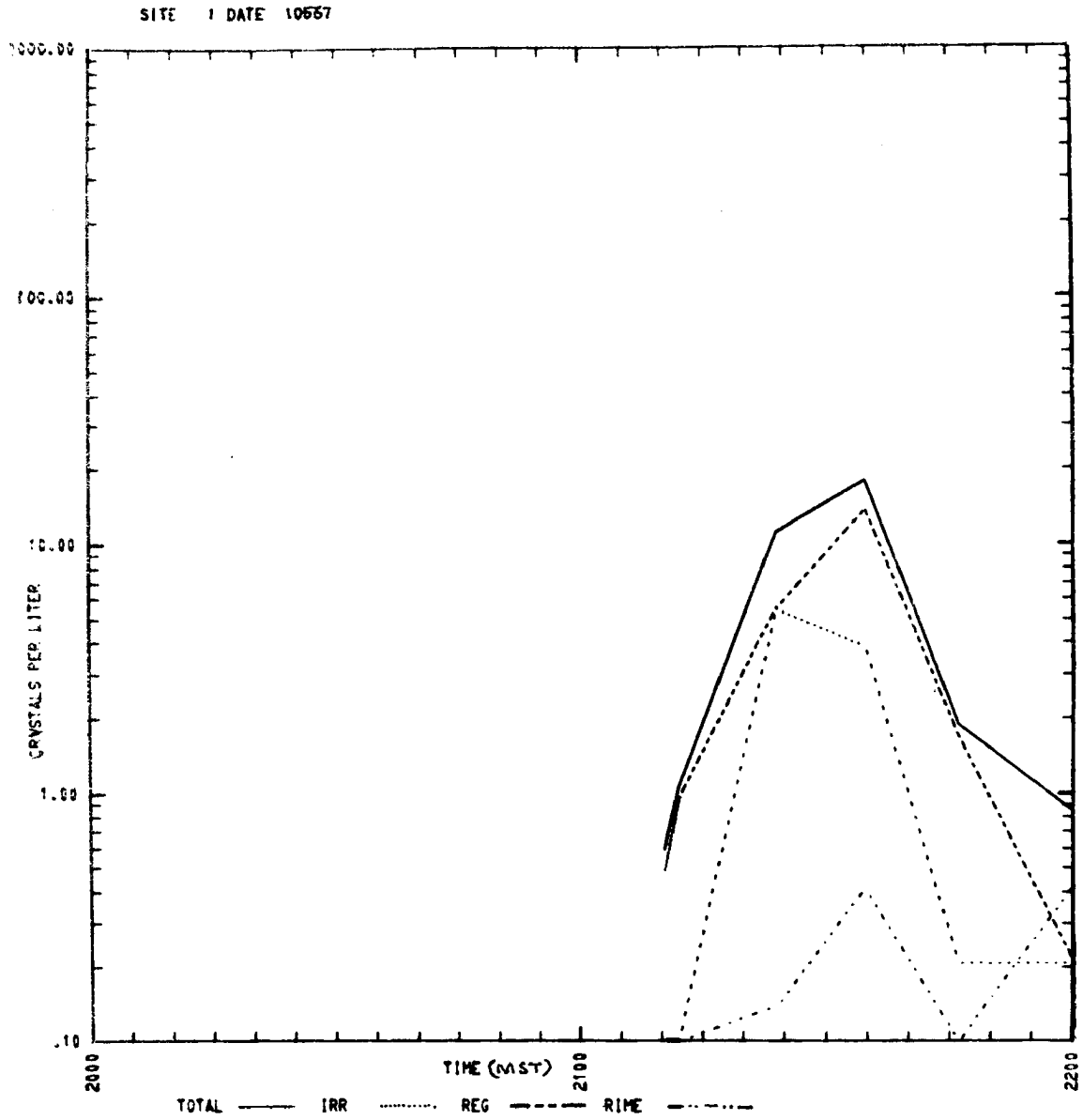


Figure 9. Typical snow crystal concentrations plotted against time, HAO, Climax, Colorado, 5 January 1967

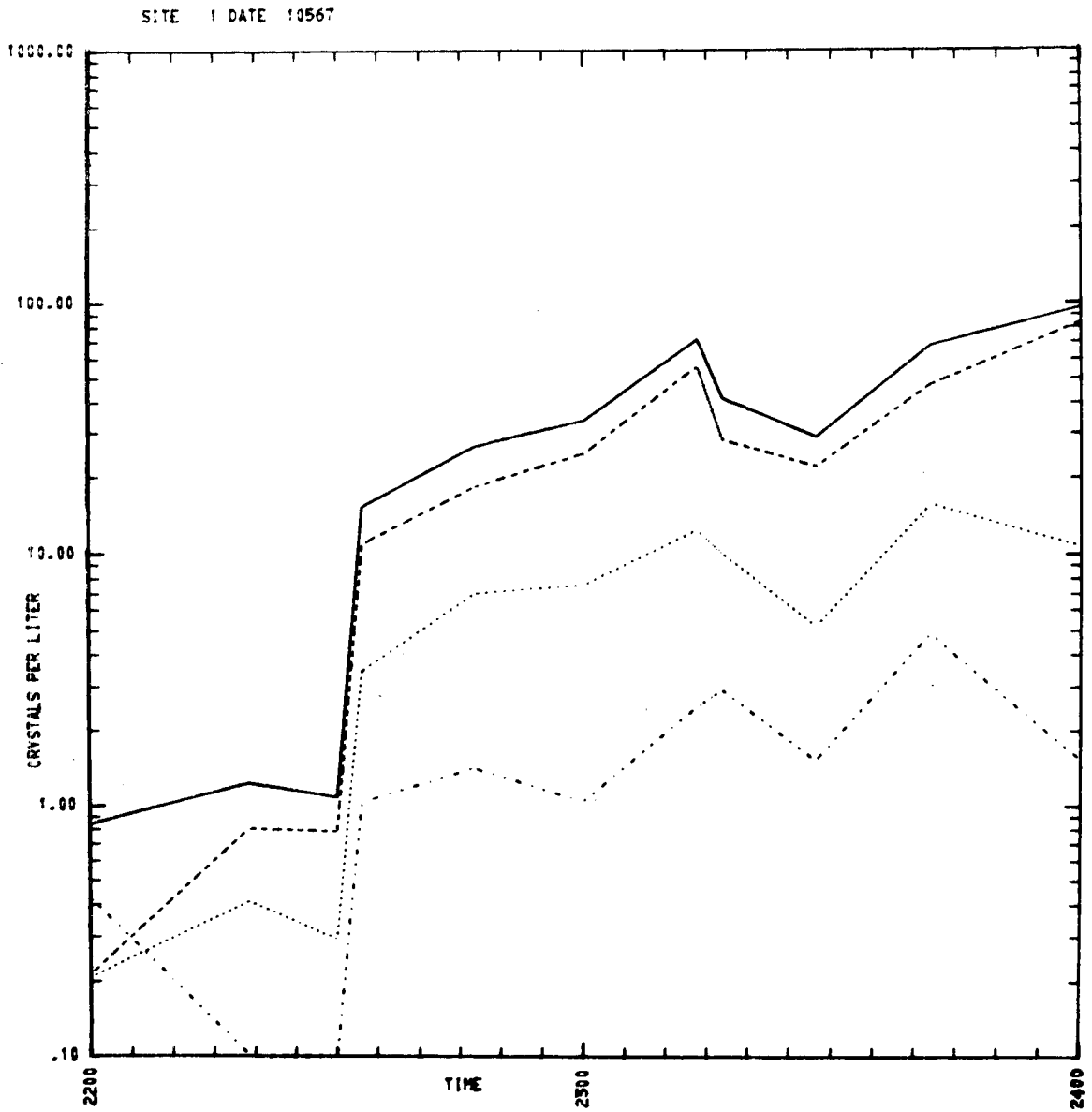


Figure 9. Continued

The consistency obtained with the analysis procedure is illustrated in Figure 10. Three continuous snowfall replicators operating in close proximity produced similar total crystal concentrations. The replicators were located within a distance of 7 km. It is seen that the total concentrations generally follow the same trends. The variability is primarily due to the intensity fluctuations in the snowfall at the individual sites. All observations for the period agree within a factor of 2.5 except one observation at HAO. This single higher observation probably represents a shower or "burst" of crystals which did not pass the other sites.

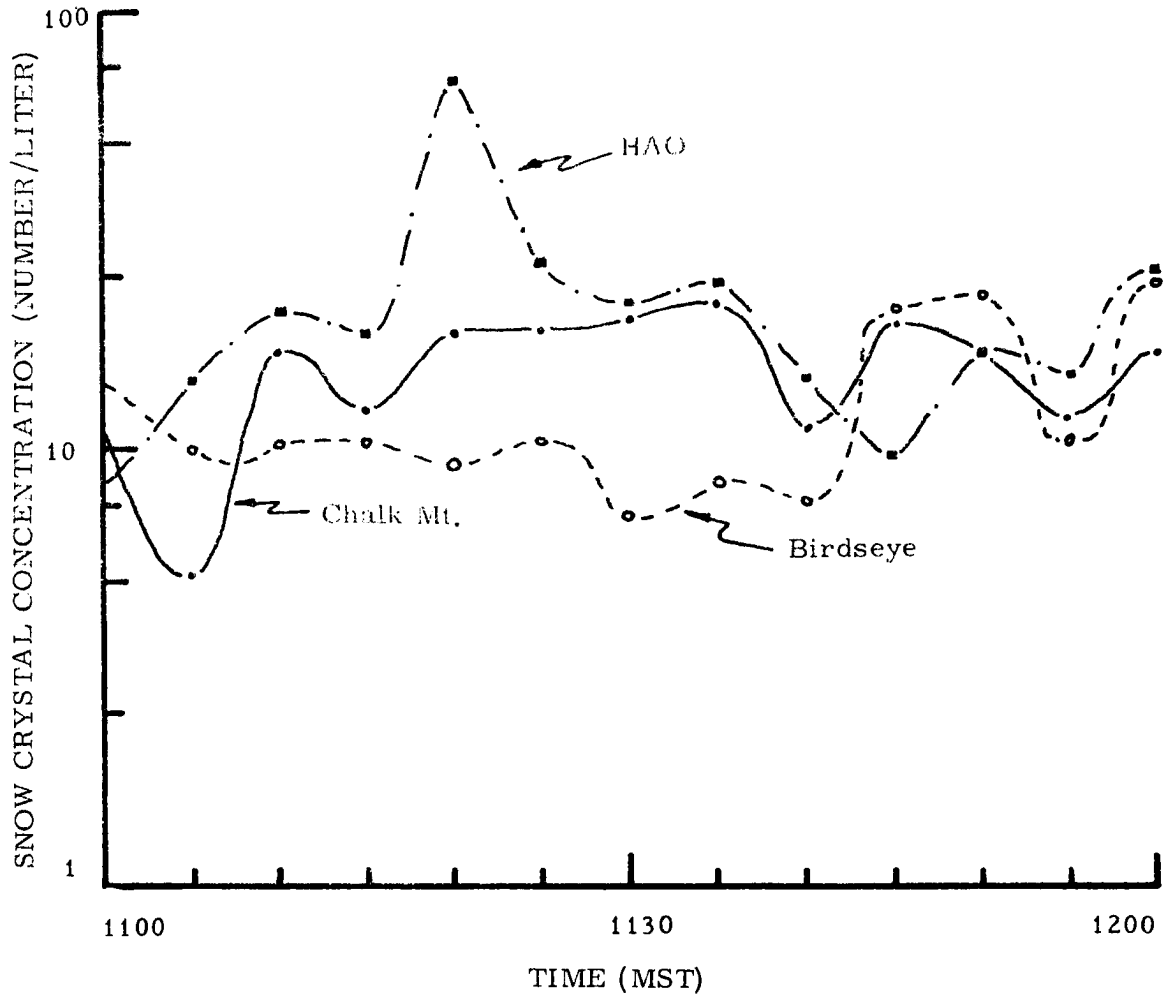


Figure 10. Comparison of total snow crystal concentrations observed by three simultaneously-operating replicators, Climax, Colorado, 27 December 1966

DATA AND ANALYSIS

Simultaneous snow crystal and ice nuclei measurements were made in only a few snowstorms at Climax during the winter of 1965-66. During the winter of 1966-67, these measurements were routine. The 1965-66 data however was the most readily available for this report. Only the most complete data for one unseeded and one seeded snowfall period is presented in detail.

Unseeded Orographic Snowfall

A large Pacific storm system moved onshore 7 February 1966, producing a strong southwest flow over Climax. By extrapolating between Denver and Grand Junction Radiosonde data, the 1700 MST 500 mb height and temperature at Climax were 5560 m and -23C. On the morning of the 8th, the trough deepened over Climax with the flow changing to a more southerly direction. The 0500 MST 500 mb temperature remained constant at -23C (dew point -25C) and the height dropped to 5460 m. The monitored snowfall period within the snowstorm started at 0630 MST with the surface temperature at -4C and the 500 mb temperature at -23C. The sampling period ended at 1215 MST with the surface and 500 mb temperatures having dropped to -8C and -25C (dew point -27C) respectively. During the snowfall period, the southerly flow veered toward the west. By 1700 MST, the

500 mb height and temperature had lowered to 5380 m and -27C (dew point -28C). The air mass from the southwest was near water saturation at all levels (temperature-dew point spread from the soundings less than or equal to 2C) providing moisture conditions suitable for a continuous cloud between the observing surface (3530 m) and the average 500 mb height (5440 m). The average tops of the cloud system are assumed to have been approximately at the 500 mb level (Furman, 1967).

The snowfall replicator was operated continuously throughout the six-hour snowfall period and concentrations were computed at regular intervals from the sample. The ice nuclei concentrations were also obtained at the same regular intervals.

Table 1 lists this simultaneous snow crystal and ice nuclei concentration data. From the total concentrations of snow crystals, the concentrations of crystals with $T_f \geq -20C$ is calculated. This concentration is obtained by summing the concentrations of snow crystal types with $T_f \geq -20C$ within the total concentration. Snow crystal concentrations are compared to the ice nuclei concentrations which have $T_a \geq -20C$. Emphasis is not placed on the individual observations because of the time lag between the crystal formation in the cloud and the ice nuclei activation in the Bigg-Warner counter at the mountain top. Instead, the data is used to compare the mean snow crystal concentration forming at $T_f \geq -20C$ and the mean ice

TABLE 1

SNOW CRYSTAL AND ICE NUCLEI CONCENTRATIONS,
 HAO, Climax, Colorado, 8 February 1966 (number/liter)

Time (MST)	Snow Crystals		Ice Nuclei
	Total	$T_f > -20C$	$T_a > -20C$
0630	15.05	0.30	0.50
0645	16.33	2.50	0.30
0655	37.07	2.07	0.60
0705	35.86	2.16	0.40
0710	36.65	1.57	1.00
0720	21.44	1.51	0.10
0735	16.25	1.61	0.05
0755	83.92	3.50	0.90
0805	23.61	0.11	0.50
0810	60.08	1.49	0.30
0820	40.42	1.26	0.05
0835	21.97	0.86	0.05
0845	59.28	2.58	0.20
0905	13.49	1.30	0.05
0915	19.65	0.60	0.05
0920	8.97	1.57	0.20
0935	17.48	1.74	1.20
0950	22.40	1.60	0.60
1000	12.13	0.70	0.70
1010	3.69	0.54	0.20
1020	4.70	0.80	0.05
1035	18.57	1.43	0.30
1045	10.00	0.61	0.10
1055	8.13	0.81	0.50
1105	17.13	0.84	0.10
1115	8.09	0.53	0.30
1140	5.58	0.48	0.05
1150	7.55	0.87	2.40
1200	7.55	0.91	0.20
1215	15.14	1.30	0.05
	$\bar{X} = 22.30$	$\bar{X} = 1.30$	$\bar{X} = 0.40$
	S = 18.70	S = 0.76	S = 0.50

nuclei concentration activated at $T_a \geq -20C$, for the entire observational period. The means (\bar{X}) and standard deviations (S) are presented in Table 1.

The variability of the snow crystal concentrations during a portion of the snowfall period is illustrated in Figure 11. The regular crystal concentration plot is the same as the crystal concentrations with $T_f \geq -20C$.

The ice nuclei concentrations are consistently lower than the snow crystal concentrations, as noted from Table 1 and verified by the following analysis. The snow crystal and ice nuclei concentrations in Table 1 with T_f and $T_a \geq -20C$ are presented in the 2 x 2 contingency tables in Table 2. The upper contingency table is constructed from the observed data as shown in Table 1. The pooled median (0.60) for the two samples was determined. The individual crystal and nuclei observations with values greater or less than 0.60 were grouped around this value. The groups were summed to produce the concentrations presented in the table. Next, a χ^2 test for independence was applied (Snedecor, 1956). The test was significant:

$$P(\chi^2 \geq 15.81) < 0.001$$

This result illustrates the concentration pairs above and below the median may not be samples from equal populations.

The lower contingency table in Table 2 is constructed from the same data in Table 1 by multiplying each nuclei concentration

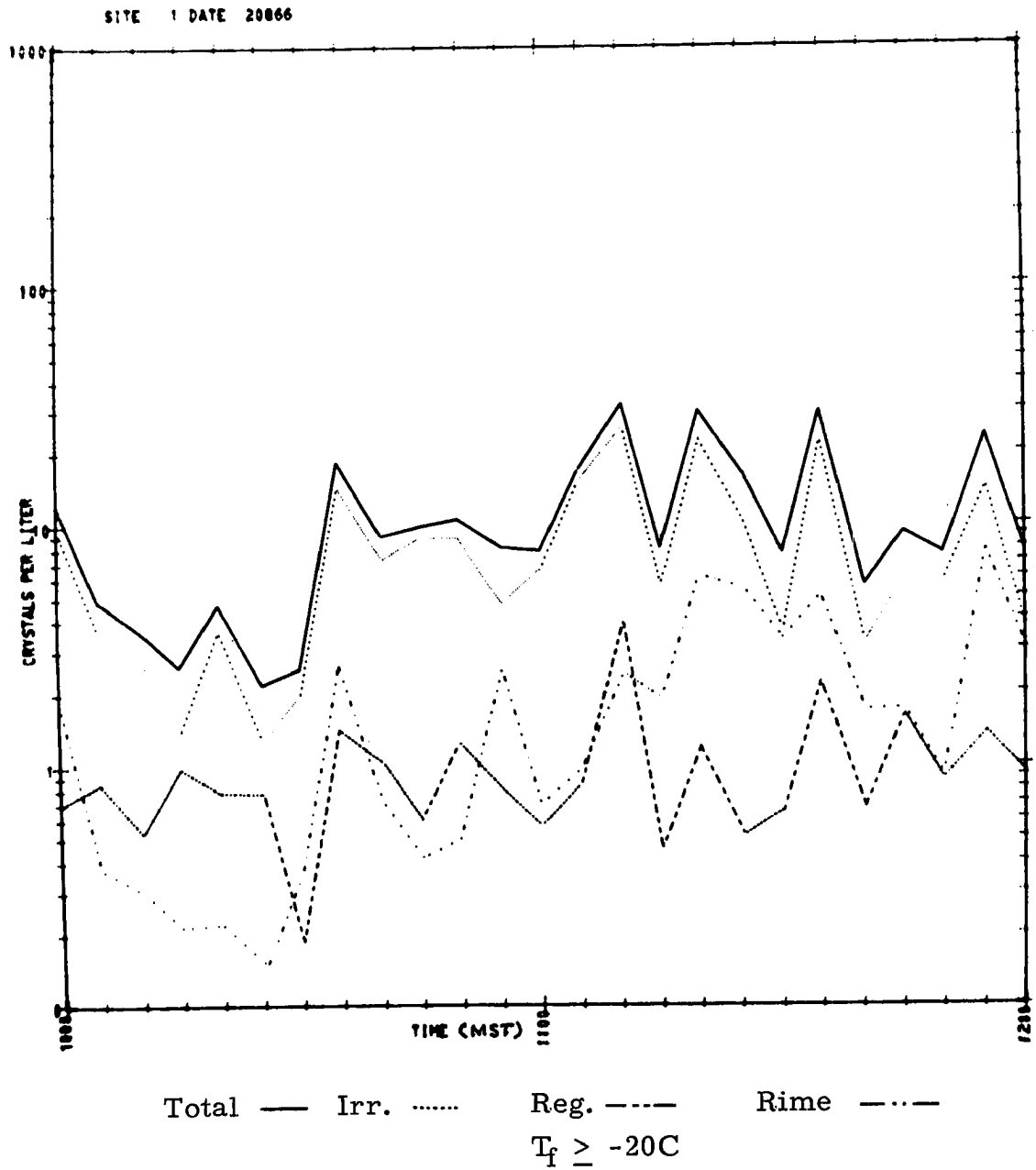


Figure 11. Snow crystal concentrations, HAO, Climax, Colorado, 8 February 1966

TABLE 2

CONTINGENCY TABLES FOR THE 8 FEBRUARY 1966
SNOW CRYSTAL AND ICE NUCLEI CONCENTRATIONS

Original Data			
Concentrations			
	Crystal	Nuclei	
Concentration below Pooled Median	a 2.56	b 6.70	9.26
Concentration above Pooled Median	c 35.59	d 5.00	40.59
	38.15	11.70	n 49.85

$$\chi^2_{1 \text{ d.f.}} = \frac{n (ad - bc)^2}{(a + b)(c + d)(a + c)(b + a)} = 15.81$$

$$P(\chi^2 \geq 15.81) < 0.001$$

Modified Data			
Concentrations			
	Crystal	Nuclei (x3.5)	
Concentrations below Pooled Median	8.96	9.41	18.37
Concentrations above Pooled Median	29.19	30.80	59.99
	38.15	40.21	78.36

$$\chi^2_{1 \text{ d.f.}} \sim 10^{-4}$$

$$P(\chi^2 \geq 0.0001) > 0.95$$

observation by 3.5--the reported average factor in the literature required to convert the Bigg-Warner expansion chamber readings to those obtained with the diffusion chamber. The concentrations are again grouped around the pooled median (1.05). The χ^2 test for independence in this case is now significant:

$$P(\chi^2 \geq 10^{-4}) > 0.95$$

This result indicates that the populations of the two samples may be similar. It appears, therefore, that the average of the reported factor difference between the Bigg-Warner expansion and diffusion chambers (3.5) is also reasonable for equating the expansion chamber observations to the corresponding snow crystal concentrations from the cloud.

Seeded Orographic Snowfall

A seeded orographic snowstorm occurred at Climax on 11 April 1966. It was not a major Pacific storm, instead, a short-wave perturbation moving through a zonal westerly flow. On the 10th, the major long-wave troughs were over the Pacific and Atlantic Coasts with a weak ridge between them. The short-wave perturbation was imbedded in the Pacific trough. The 500 mb height, temperature, and wind over Climax on the 10th were 5750 m, -18C, and westerly. The short-wave trough was over Climax on the afternoon of the 11th. The 1700 MST 500 mb height was 5680 m; the temperature and dew point

were -21 and -22C; and the wind was west-northwest (WNW) at 15 m per second. The snowfall period monitored started at 1600 and ended at 1800 MST. The surface temperature was constant at -2C. Silver iodide generators were in operation at Tennessee Pass and Redcliff two hours before the investigated snowfall period. Tennessee Pass is approximately 10 km to the west of Climax. Redcliff is approximately 15 km to the northwest as illustrated in Figure 1. The assumption is made that the WNW wind caused a major portion of each AgI plume to reach the Climax area. The consistent westerly wind with nearly saturated conditions at 500 mb indicates a solid orographic cloud system formed over Climax.

Table 3 lists the snow crystal and ice nuclei concentrations taken during the snowfall period on 11 April 1966. Simultaneous crystal and nuclei observations were not obtained. The mean (\bar{X}) and standard deviation (S) of the nuclei observations indicate little variability. Thus, nuclei concentrations are assumed approximately constant through the period. The snow crystal concentrations are variable as illustrated in Figure 12. The time periods with no snow crystals ($T_f \geq -20C$) represent discontinuities in the lower cloud system.

It is not feasible to analyze the data in Table 3 by the contingency procedure used for the unseeded storm because the value of the pooled median for the crystal and nuclei observations is 1.83.

There is no nuclei concentration in Table 3 less than this value, so one box in the contingency table would have a value of zero. This value would cause the χ^2 independence test to result in significance. If the nuclei concentrations were multiplied by 3.5, the test would still be significant. Thus, the value of 3.5 does not explain the higher nuclei concentrations.

DISCUSSION

Unseeded Orographic Snowfall

A schematic diagram of the unseeded orographic cloud system over Climax during the investigated snowfall period on 8 February 1966 is presented in Figure 13. The synoptic parameters are the mean values for the snowfall period since no large variations occurred during the period. The cloud system is simplified in this manner so the Bigg-Warner expansion counter can be used to simulate in-cloud temperature conditions. The nuclei concentrations measured at an activation temperature of -20°C in the counter--when multiplied by the 3.5 adjustment factor--are assumed to approximate the concentrations in a column of air extending through that portion of the cloud with temperatures greater than or equal to -20°C . Likewise, the concentrations of snow crystals with formation temperatures at or above -20°C , when measured at the ground, are assumed to have formed between these corresponding levels in the cloud. Thus, the crystal and nuclei concentrations in Table 1 with T_f and $T_a \geq -20^{\circ}\text{C}$ can be related. The variable concentrations and the inherent time lag between the simultaneous observations allows only the mean concentrations to be related.

The relationship between the snow crystal and ice nuclei concentrations in this snowfall period might be preliminarily inferred

from the simplification of the orographic cloud system represented in Figure 13. The nuclei concentrations measured in the inactive natural nuclei layer on the mountain top are used to represent the in-cloud concentrations. As a result, it is not unreasonable to assume that snow crystal concentrations--which formed at temperatures at or above -20°C in the cloud, when measured at the ground--formed from the equivalent nuclei concentration measured at $T_a = -20^{\circ}\text{C}$ in the nuclei counter. The mean values in Table 1 with T_f and $T_a \geq -20^{\circ}\text{C}$ support a hypothesis that each ice nucleus formed one snow crystal. The mean snow crystal concentration of 1.3 per liter is nearly equal to the mean ice nuclei concentration of 1.4 per liter when the original 0.40 value is multiplied by the 3.5 adjustment factor. Likewise, the median crystal and nuclei ($\times 3.5$) concentrations were approximately equal at 1.3 and 0.90 per liter, respectively.

Additional data is available to show that snow crystal and ice nuclei concentrations are nearly equal at the ground. For example, an unseeded snowfall period between 1752 and 2058 MST on 19 April 1966 at HAO was investigated in the same manner as the 8 February 1966 storm. The means of the snow crystal and ice nuclei concentrations with T_f and $T_a \geq -20^{\circ}\text{C}$ are also in fairly good agreement at 2.8 and 5.9 per liter, respectively, incorporating the factor of 3.5 in the nuclei concentrations. The standard deviations of the crystal

cloud. It is difficult however to determine the total concentration of either nuclei component, because their activation layers overlap in the cloud, and the air sample at the ground contains both components. If nuclei concentrations were taken at $T_a = -12\text{C}$, they would probably indicate a portion of the total artificial nuclei concentration since the natural nuclei do not activate at temperatures warmer than approximately -12C (Schaefer, 1951). The artificial AgI nuclei used at Climax activate at temperatures as warm as approximately -8C (Grant and Mielke, 1965). For example, on 11 April 1966, before the AgI plume reached Climax, the average nuclei concentrations for $T_a = -12\text{C}$ were zero. During the seeded snowfall period, the nuclei concentrations at $T_a = -12\text{C}$ increased to 0.4 per liter. The 0.4 concentration, while too low to support a firm conclusion, indicated the AgI nuclei concentration active at $-12\text{C} \leq T_a \leq -8\text{C}$.

A relationship between the snow crystal and ice nuclei concentrations measured at the ground in seeded snowfall is more difficult to develop than for unseeded snowfall. The difficulty exists because the AgI plume in Figure 14 probably should not be assumed uniformly diffused through the cloud volume. It is argued that if the generators are located sufficiently distant upwind of the orographic barrier, mixing motions may diffuse the plume uniformly throughout the cloud. If this is the case, the hypothesis for unseeded cloud systems indicating equality between the snow crystal and ice nuclei

concentrations would be reasonable. If however the plume did not uniformly mix throughout the cloud, this hypothesis would not be substantiated.

Under this condition, the plume possibly would not be totally activated in the cloud, but may be totally activated in the Bigg-Warner expansion chamber. For example, if the plume diffuses as illustrated in Figure 14, nuclei concentrations activated at -20C in the counter might be greater than the concentrations of snow crystals precipitating from the cloud. The snow crystal concentration with $T_f \geq -20\text{C}$ may not be forming on the total AgI nuclei concentration because the majority of the plume does not reach the -20C level. This hypothesis is tested using the mean snow crystal and ice nuclei concentrations in Table 3 with T_f and $T_a \geq -20\text{C}$. The ice nuclei concentrations, when multiplied by 3.5, are a factor of nearly 11 greater than the snow crystal concentrations; 20.3 and 1.9 per liter, respectively. Likewise, the median ice nuclei concentration ($\times 3.5$) was a factor of approximately 28 greater than the median snow crystal concentration; 25.0 and 0.9 per liter, respectively.

Another seeded snowfall period was monitored for three hours on 17 March 1966. The mean snow crystal and ice nuclei concentrations with T_f and $T_a \geq -20\text{C}$ were 0.6 and 5.6 per liter, respectively, incorporating the factor of 3.5 in the nuclei mean.

They differed by a factor of 9, although the snowfall was variable. The crystal and nuclei standard deviation were 0.8 and 4.5 per liter. Likewise, the median nuclei concentrations ($\times 3.5$) were 3.8, differing by a factor of 38 from the median crystal concentration of 0.1 per liter.

Although the snow crystal and ice nuclei concentrations were highly variable in the two seeded snowfall periods, there are distinct differences between the concentrations. It is apparent the nuclei concentrations are at least an order of magnitude greater than the crystal concentrations. A specific value cannot be inferred because of the variability in the existing snowfall conditions. These results illustrate that the AgI plume probably was not completely diffused throughout the cloud, thus not totally activated. Furthermore, the snow crystal concentrations are within the same order of magnitude as the unseeded cases regardless of the apparent order of magnitude increase in the nuclei concentrations at the ground in the seeded snowfall. From this limited amount of data, it is clear the snow crystal and ice nuclei concentrations at the ground are not equal for seeded cases investigated. Consequently, it appears that in-cloud crystal and nuclei concentrations cannot be inferred from nuclei observations at the ground in seeded snowfall at Climax.

Total Ice Nuclei and Snow Crystal Concentrations

The total ice nuclei concentrations activated and the total snow crystal concentrations formed at all temperatures in an

orographic cloud system can be considered using the simplified cloud represented in Figure 3. If a sample of air is activated in the Bigg-Warner expansion chamber at the temperature of cloud tops, the nuclei concentration is assumed to nearly represent the concentration of active nuclei in the cloud from the threshold activation level to the cloud-top level. Likewise, if the snow crystal concentrations with T_f greater than or equal to cloud-top temperature are summed, this sample at the ground closely represents the total concentration in the cloud. The relationship of these nuclei and crystal concentrations have been investigated.

Table 4 illustrates the total nuclei and crystal concentrations for seeded and unseeded snowfall periods. Considerable variability exists between the individual values as noted earlier. In Table 4, the variability in the total snow crystal concentrations may be a result of the crystal interpretation problem inherent with the identification of irregular crystals. The cloud-top temperatures (near the 500 mb temperature, according to Furman, 1967) averaged -25°C for all snowfall periods; therefore, the ice nuclei concentrations with $T_a \geq -26^{\circ}\text{C}$ can be considered to nearly represent the total concentration in the cloud.

The mean total snow crystal concentration ($12.85 \ell^{-1}$) is greater than the ice nuclei concentration ($3.95 \ell^{-1}$) by a factor of 4 in the unseeded storms. If the factor of 3.5 is incorporated in the

TABLE 4

TOTAL SNOW CRYSTAL AND
ICE NUCLEI CONCENTRATIONS

Date	Site	Time Period (MST)	Seeded	500 mb Temp. (° C)	Total Crystal Conc. (n/l)		Nuclei Conc. (n/l) $T_a \geq -26C$	
					\bar{X}	S	\bar{X}	S
2-8-66	HAO	0630-1215	No	-24	22.30	18.70	1.90	-
3-17-66	HAO	0730-1040	Yes	-28	5.09	5.37	8.41	-
4-11-66	HAO	1600-1800	Yes	-21	11.56	13.47	10.80	-
4-19-66	HAO	1752-2058	No	-26	3.40	3.00	6.00	-
-Averages-								
			No	-25	12.85	10.85	3.95	-
			Yes	-25	8.33	9.42	9.65	-

nuclei concentrations, the mean total crystal and nuclei concentrations are again in good agreement, 13.0 and 14.0 per liter, respectively. This result suggests that total ice nuclei and snow crystal concentrations may be equal in these unseeded orographic snowfall periods.

The mean total snow crystal concentration ($8.33 \ell^{-1}$) for the seeded storms is approximately equal to the ice nuclei concentration with $T_a \geq -26\text{C}$ ($9.65 \ell^{-1}$). When the factor of 3.5 is incorporated, the mean nuclei concentration increases to 33.8 per liter. They differ by a factor of 4, but not by as large a factor as the cases with T_f and $T_a \geq -20\text{C}$, again possibly indicating higher nuclei concentrations near the ground. This decrease in the magnitude of the factor might be expected because the concentrations of active natural ice nuclei increase substantially between -20 and -26C .

The total crystal and nuclei concentrations in the cloud may be reasonably inferred from nuclei concentrations activated at the cloud-top temperature in the unseeded snowfall cases, but not in the case when artificial nuclei are superimposed on the system. It must be emphasized that these and the previous results are applicable to mountain-top observations in the Central Colorado Rockies during winter and are based on a very limited sample.

SUMMARY AND CONCLUSIONS

Snow Crystal and Ice Nuclei Concentrations

Ice nuclei and snow crystal concentrations were measured simultaneously at the ground in two unseeded and two seeded orographic snowfall periods at Climax, Colorado. From these observations, the snow crystal and ice nuclei concentrations with the same formation and activation temperatures were compared.

An average factor of 3.5 has been determined by Warner and Newnham (1958) in comparing the ice nuclei concentrations obtained with the Bigg-Warner expansion-type ice nuclei counter to those obtained with a Bigg-Warner diffusion chamber. Now, this same factor appears realistic in comparing the Bigg-Warner expansion chamber to snow crystal concentrations from unseeded orographic cloud systems.

The mean snow crystal and ice nuclei concentrations, with formation and activation temperatures at or above -20°C in the investigated unseeded orographic cloud systems, were approximately equal. Likewise, the total concentrations active at all temperatures to -25°C in these same cloud systems were approximately equal. Thus, in-cloud crystal and nuclei concentrations were reasonably inferred from nuclei measurements at the ground.

The mean snow crystal and ice nuclei concentrations differed significantly for temperatures at or above -20°C in the investigated seeded orographic cloud systems. Likewise, the total crystal and nuclei concentrations active at all temperatures to -25°C differed significantly. The variability of the snowfall did not allow a mean difference to be determined, however the nuclei concentrations appeared greater than the crystal concentrations, by at least an order of magnitude. Consequently, nuclei concentrations measured at the ground in seeded snowfall did not represent in-cloud conditions. The larger nuclei concentrations are probably a result of non-uniform mixing of the artificial nuclei plume, producing much higher concentrations near the ground than in the cloud.

The equality of snow crystal and ice nuclei concentrations in unseeded orographic snowfall supports the observation by Kumai (1951) which states each snow crystal contains one solid nucleus. Isono (1965) has found a similar relationship between the concentrations of graupel and ice nuclei at the bases of unseeded thunderstorms over Japan.

These preliminary crystal and nuclei concentration relationships are to be considered tentative statements because they are based on a limited sample. Lack of precedence in theory and technique hindered the more precise interpretation of the crystal and nuclei relationships. Finding these concentrations to be within the same order of magnitude is considered remarkable.

Instrumentation

The continuous snowfall replicator has improved the procedure for taking Formvar snow crystal replicas at Climax, Colorado (Grant, 1965a). The improvement primarily involves the even coating of the Formvar solution applied to the 35 mm film base. The even coating and the slow time for solution hardening suppresses "blush" which sometimes masks the samples taken with other Formvar replication techniques (Averitt and Ruskin, 1967). The instrument is not able to replicate crystals in temperatures warmer than -1C. Replication of rainfall is, therefore, not possible.

The procedure for computing snow crystal concentrations from the continuous snowfall replicator data appears realistic because these concentrations are comparable to simultaneously-measured ice nuclei concentrations. The Bigg-Warner expansion chamber measures the concentrations of the nuclei on which snow crystals form. The replicator is used to determine the resulting concentrations of snow crystals. Finding these concentrations to be within the same order of magnitude is submitted as possible evidence for the validity of the procedure for computing snow crystal concentrations.

RECOMMENDATIONS

Measurements from the kite-borne cloud particle and ice nuclei samplers--developed at Colorado State University to be flown in orographic cloud systems--may verify the ground observations in this paper. The in-cloud measurements of water droplet, ice crystal, and ice nuclei concentrations, coupled with the ground measurements of snow crystal and ice nuclei concentrations, may clarify the precipitation processes in the orographic cloud systems.

Many of the questions presented in this report may be resolved by the careful analysis of an increasing sample of snow crystal and ice nuclei concentrations now becoming available.

REFERENCES

REFERENCES

- Averitt, J. and R. Ruskin, 1967: Cloud particle replication in Stormfury tropical cumulus. J. Appl. Meteor. 1, 89-94.
- Bergeron, T., 1949: The problem of artificial control of rainfall on the globe. Tellus, 1, 32-50.
- Bourquard, A. D., 1963: Ice nucleus concentrations at the ground. J. Atmos. Sci., 5, 386-391.
- Bowen, E. G., 1956: The relation between rainfall and meteoric showers. J. Meteor., 13, 142-151.
- Bryant, G. W., and B. J. Mason, 1960: Photolytic de-activation of silver iodide as an ice-forming nucleus. Quart. J. Royal Meteor. Soc., 86, 354-357.
- Droessler, E., 1965: The distribution and origin of atmospheric ice nuclei. Proc. of the Int. Conf. of Cloud Physics. Tokyo and Sapporo, Japan, 131-136.
- Fletcher, N. H., 1958: Time lag in ice crystal nucleation in the atmosphere. Bull. Obs. Puy de Dome, 1, 11-18.
- _____, 1962: The Physics of Rainclouds, Cambridge University Press, 347 pp.
- Furman, R. W., 1967: Radar characteristics of wintertime storms in the Colorado Rockies. M. S. Thesis, Colorado State University, Dept. of Atmos. Sci., Fort Collins, Colorado.
- Grant, L. O., and R. A. Schlessener, 1961: The occurrence and variability of ice-forming nuclei during the hail season in N. E. Colorado as measured at 11,300 ft m. s. l. at an up-wind mountain station. Nubila, 2, 21-27.
- _____, and P. W. Mielke, Jr., 1965: Randomized cloud seeding experiment at Climax, Colorado. Proc. of the Fifth Berkeley Symposium on Mathematical Statistics and Probability, Weather Modification Section, Berkeley, California, December 27-28, 1965, 15 pp.

- Grant, L. O., 1965a: Shapes and concentrations of snow crystals observed at 11,300 ft m. s. l. near Climax, Colorado. Presented at 244th National Meeting, AMS on Cloud Physics and Severe Local Storms. October 18-22, 1965, Reno, Nevada. (On file, Colorado State University, Dept. of Atmos. Sci., Fort Collins, Colorado).
- _____, and R. L. Steele, 1966: The calibration of silver iodide generators. Bull. Am. Meteor. Soc., 9, 713-717.
- Gunn, R., and G. Kinzer, 1949: The terminal velocity of fall for water droplets in stagnant air. J. Meteor., 6, 243-248.
- Henderson, T., 1965: Tracking silver iodide nuclei under orographic influence. Presented at 244th National Meeting of the AMS on Cloud Physics and Severe Local Storms. October 18-22, 1965, Reno, Nevada. (On file, Atmospherics, Inc., Fresno, California).
- Hindman, E. E. II, 1964: Continuous sampler for settling particles. J. de Recherches Atmosphériques, 1, 29-35.
- _____, 1966: The phase change in an artificial supercooled cloud upon heterogeneous and homogeneous nucleation. J. Atmos. Sci., 1, 67-73.
- _____, and R. F. Reinking, 1966a: Analysis of continua of snow crystal replicas from Colorado mountain and Yellowstone Park snowfall. Presented at 6th Western Meeting, AGU, September 7-9, 1966, University of California at Los Angeles, California, 9 pp. (On file, Colorado State University, Dept. of Atmos. Sci., Fort Collins, Colorado).
- _____, and R. L. Rinker, 1967: Continuous snowfall replicator. J. Appl. Meteor., 1, 126-133.
- Hobbs, P. V., 1965: The aggregation of ice particles in clouds and fogs at low temperatures. J. Atmos. Sci., 3, 296-300.
- Hosler, C. L., D. C. Jensen, and L. Goldshlak, 1957: On the aggregation of ice crystals to form snow. J. Meteor., 14, 415-420.
- _____, and R. E. Hallgren, 1961: Ice crystal aggregation. Nubila, 1, 13-19.

- Isono, K., 1955: On ice crystal nuclei and other substances found in snow crystals. J. Meteor., 12, 456-462.
- _____, 1965: Variation of ice nucleus concentration in the atmosphere and its effect on precipitation. Proc. of the Int. Conf. on Cloud Physics. Tokyo and Sapporo, Japan, 150-154.
- Kassander, A. R., L. L. Sims, and J. E. MacDonald, 1957: Observation of freezing nuclei over the Southwestern United States. Artificial Stimulation of Rain, ed. H. Weickmann and W. Smith, London: Pergamon Press, 393-394.
- Kepler, J., 1611: On the Six-Cornered Snowflake. Oxford at the Clarendon Press, 1966, 50 pp.
- Klein, D. B., and G. W. Brier, 1961: Some experiments on the measurement of natural ice nuclei. Mo. Wea. Rev., 89, 263-272.
- Kumai, M., 1951: Electron-microscope study of snow crystal nuclei. J. Meteor., 8, 151-156.
- Ludlam, F. H., 1955: Artificial snowfall from mountain clouds. Tellus, 7, 277-290.
- MacCready, P. B., Jr., 1962: The continuous particle sampler at the Puy de Dome comparison conference. Bull. Obs. Puy de Dome, 1, 19-30.
- _____, and C. J. Todd, 1964: Continuous particle sampler. J. Appl. Meteor., 4, 450-460.
- Magono, C., 1962: The temperature conditions for the growth of natural and artificial snow crystals. J. Meteor. Soc. of Japan. 4, 185-192.
- _____, and S. Tazawa, 1966: Design of "snow crystal sondes." J. Atmos. Sci., 23, 618-625.
- Nakaya, U., 1954: Snow Crystals. Harvard University Press, 508pp.
- Power, B. A., P. W. Sommers, and J. d'Avignon, 1964: Snow crystal forms and riming effects as related to snowfall density and general storm conditions. J. Atmos. Sci., 3, 300-305.

- Reynolds, S. E., W. Hume, and M. McWhirter, 1952: Effects of sunlight in ammonia on the action of AgI particles as sublimation nuclei. Bull. Am. Meteor. Soc., 33, 26-30.
- Schaefer, V. J., 1941: Method of making replicas of snow flakes, ice crystals, and other short-lived substances. Museum News, 19, 11-14.
- _____, 1951: Snow and its relationship to experimental meteorology. Compendium of Meteorology, AMS, 221-234.
- _____, 1954: The concentration of ice nuclei passing the summit of Mt. Washington. Bull. Am. Meteor. Soc., 7, 310-314.
- _____, 1964: Preparation of permanent replicas of snow, frost, and ice. Weatherwise, 6, 279-287.
- Smith, E., and K. Heffernan, 1954: Airborne measurements of the concentrations of natural and artificial freezing nuclei. Quart. J. Royal Meteor. Soc., 80, 182-197.
- Snedecor, G., 1956: Statistical Methods, Iowa State University Press, 523 pp.
- Todd, C. J., 1964: A system for computing ice phase hydrometeor development. Atmospheric Research Group, Altadena, California, (ARG 64 Pa-121), 30 pp.
- Warner, J., 1957: An instrument for the measurement of freezing nucleus concentration. Bull. Obs. Puy de Dome, 2, 33-46.
- _____, and T. D. Newnham, 1958: Time lag in ice crystal nucleation in the atmosphere. Bull. Obs. Puy de Dome, 1, 1-10.

APPENDICES

APPENDIX A

Continuous Snowfall Replicator System

Operation of the Continuous Snowfall Replicator

The continuous snowfall replicator and components are illustrated in Figures 4, 5, and 6. The solution of 4% Formvar, 4% Toluene in ethylene-dichloride is placed in the reservoir tank, illustrated in Figure 5. The coating wheel is detachable to permit ease in filling and emptying. The reservoir is placed in the instrument, in Figure 4, after filling. Uncoated 35 mm film base is stored in the left-hand reel. The film is fed from this reel and through the film-guide system, passed the coating tank and sampling slit in Figure 6. The film continues through the drying length, passed the drive sprocket, and onto the take-up reel. The film rate is 3.14 inches per minute, and the sampling slit in Figure 6 is adjustable from nearly closed to 3 inches open. This variable allows exposure times to be regulated to the intensity of the snowfall. For heavy snowfall, a 1/2- to 3/4-inch opening is used, and for lighter snowfall a 1- to 1 1/2-inch opening is used.

The continuous snowfall replicator is operated in a systematic manner during the snowfall period. A "start mark" is placed on the film as the instrument is activated. Then, the date, time of mark, site, slit width, and storm conditions are recorded. At one-hour intervals,

the instrument's operation is checked. A time mark is made on the film, and this storm data is recorded at each check. The slit width is adjusted if the snowfall rate has increased or decreased from the previous check. When the snowfall period ends, a "stop mark" is written on the film, and the time - with associated storm data - is recorded. When the experiment terminates, the unused Formvar solution is poured into a container and the reservoir plus coating wheel are soaked and cleaned in ethylene-dichloride until the next operation.

The continuous snowfall replicas for the snowfall period are contained on the take-up reel. This reel is removed from the instrument and catalogued with an accompanying data sheet. Then, the data is ready for reduction.

Data Reduction System

The 35 mm film base containing the snow crystal replicas is analyzed by using the modified 35 mm film-strip projector in Figure 15 to determine crystal concentrations. The normal 5-inch lens was replaced with a 3-inch wide-angle lens¹. This lens produces a magnification of 70X when the projector is set approximately 17 feet from the screen. Figure 16 is the actual size of the scale used to measure the dimensions of the projected snow crystal

¹ 3-inch E. F. f/3.0 Luxtar L. P. Anastigmat, Viewlex, Inc., Long Island, New York.

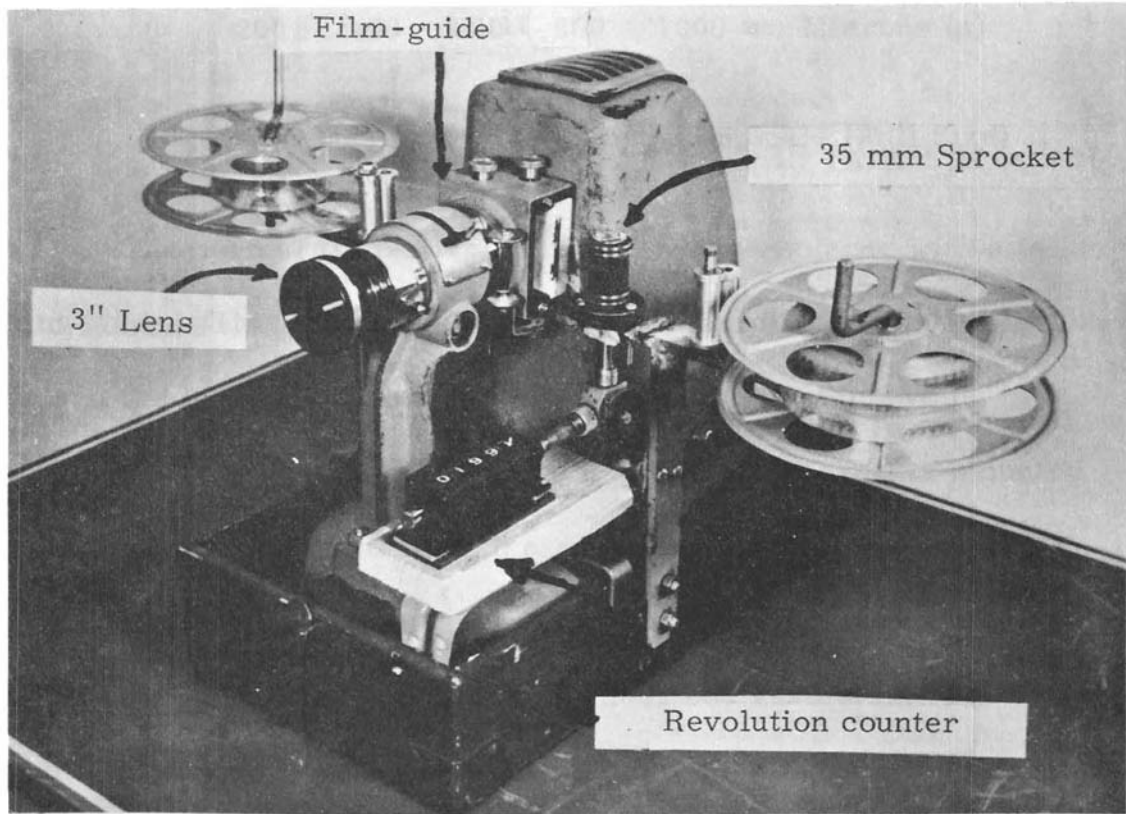


Figure 15. The snow crystal replica film-strip projector

The continuous snow crystal replica film with event times to be investigated, is projected onto a grid corresponding to 4.5 cm^2 on the film. The 4.5 cm^2 area was calculated to be the minimum area that must be observed to give a statistically significant sample. The crystal replicas are classified according to Nakaya (1954) in Figure 17 and Table 5. Nakaya's crystal type nomenclature in Figure 17 is digitized in Table 6. At a specific event time, all the crystals on the grid are counted and classified according to size and shape. Typical snow crystal replica data read from the grid is presented in Table 7. This data corresponds to the crystal concentrations in Figure 8.

Data in Table 7 was taken at the High Altitude Observatory, Climax, Colorado (site 001) on 5 January 1967 (010567). The snowfall period was between 2110 and 2400 MST and Table 7 illustrates only the first three and a portion of the final event times investigated. For example, at 2110 MST, one P1a crystal type (0311), with a length of 210μ , and one I1 crystal type (0061), with a length of 110μ , were observed on the 4.5 cm^2 grid. This same reasoning follows for the remainder of the snowfall data.

Snow crystal data is placed on IBM punch cards in the exact form as presented in Table 7. The first card is the identification card: site (3 digits, columns 1-3), date (6 digits, columns 4-9). Then each observed snow crystal type and size is placed on a

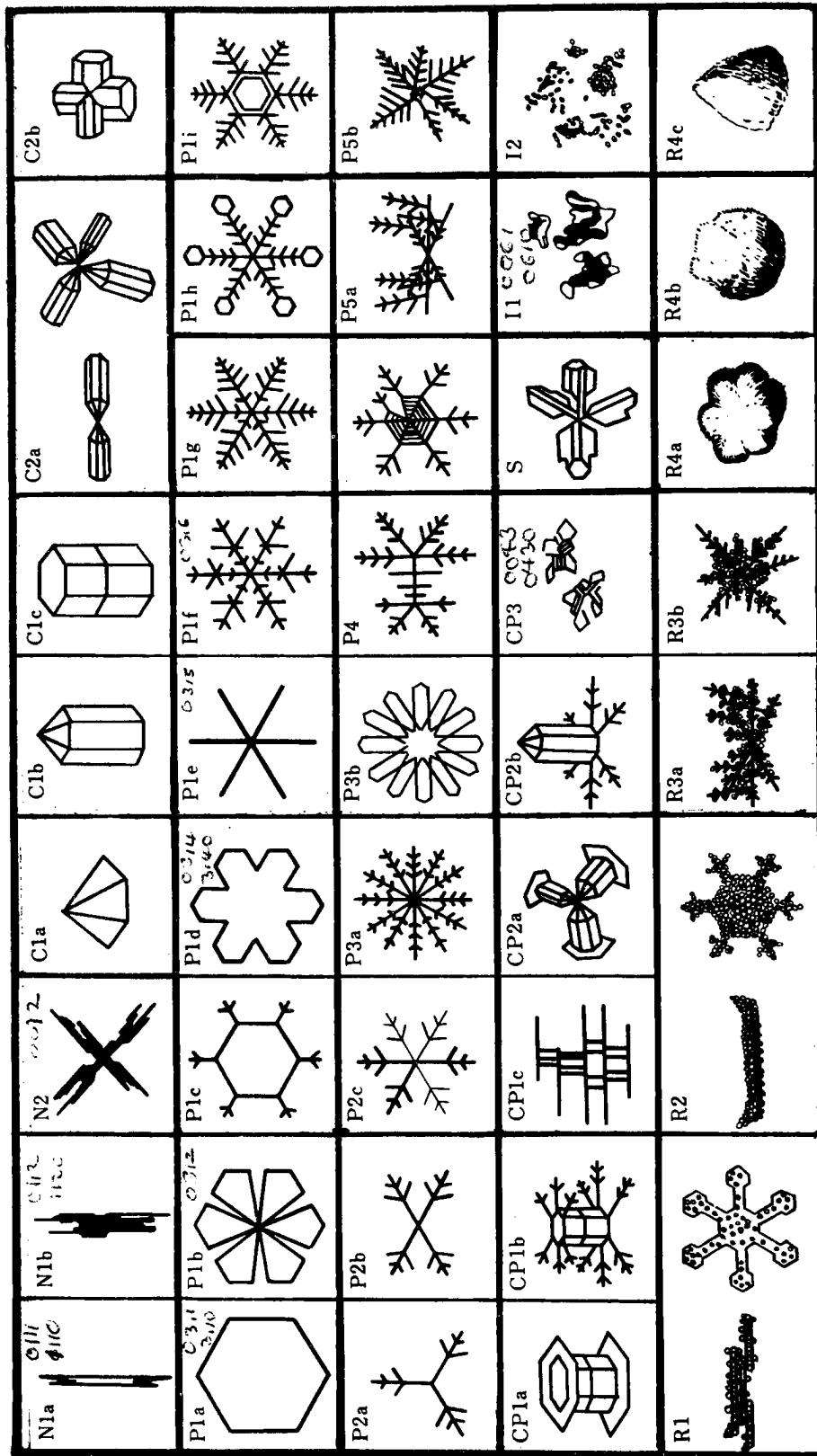


Figure 17. General classification of snow crystals, sketches [from Nakaya (1954)]

TABLE 5
 GENERAL CLASSIFICATION OF SNOW CRYSTALS
 [from Nakaya (1954)]

I	N	Needle crystal	1. Simple needle	0111 a. Elementary needle 0111 0112 b. Bundle of elementary needles 0112	0111 0112
			2. Combination	0012	
II	C	Columnar crystal	1. Simple column	0211 a. Pyramid 211 0212 b. Bullet type 212 0213 c. Hexagonal column 213	211 212 213
			2. Combination	0221 a. Combination of bullets 221 0222 b. Combination of columns 222	221 222
III	P	Plane crystal	1. Regular crystal developed in one plane	0311 a. Simple plate 311 0312 b. Branches in sector form 312 0313 c. Plate with simple extensions 313 0314 d. Broad branches 314 0315 e. Simple stellar form 315 0316 f. Ordinary dendritic form 316 0317 g. Fernlike crystal 317 0318 h. Stellar crystal with plates at ends 318 0319 i. Plate with dendritic extensions 319	3
			2. Crystal with irregular number of branches	0321 a. Three-branched crystal 321 0322 b. Four-branched crystal 322 0323 c. Others 323	
			3. Crystal with twelve branches	0331 a. Fernlike crystal 331 0332 b. Broad branches 332	
			4. Malformed crystal	Many varieties 3'	
			5. Spacial assemblage of plane branches	a. Spacial hexagonal type b. Radiating type	
IV	CP	Combination of column and plane crystals	1. Column with plane crystals at both ends	0411 a. Column with plates 411 0412 b. Column with dendritic crystal 412 0413 c. Complicated capped column 413	
			2. Bullets with plane crystals	0421 a. Bullets with plates 421 0422 b. Bullets with dendritic crystals 422	
			3. Irregular assemblage of columns and plates	0043	
V	S	Columnar crystal with extended side planes		0005	
VI	R	Rimed crystal (crystal with cloud particles attached)	1. Rimed crystal 2. Thick plate 3. Graupellike snow 4. Graupel	a. Hexagonal type b. Lump type a. Hexagonal graupel b. Lump graupel c. Conelike graupel	
VII	I	Irregular snow particle	1. Ice particle 2. Rimed particle 3. Miscellaneous	0061 0062 0616	

TABLE 6

NUMERICAL SNOW CRYSTAL TYPES
[after Nakaya (1954)]

Nakaya	Numerical	Letter(s)	Number
N1a	0111	N	1
N1b	0112	C	2
N2	0012	P	3
C1a	0211	CP	4
C1b	0212	S	5
C1c	0213	I	6
C2a	0221	R	0 at the end
C2b	0222	a	1
P1a	0311	b	2
P1b	0312	c	3
P1c	0313	d	4
P1d	0314	e	5
P1e	0315	f	6
P1f	0316	g	7
P1g	0317	h	8
P1h	0318	i	9
P1i	0319		
P2a	0321		
P2b	0322		
P2c	0323		
P3a	0331		
P3b	0332		
CP1a	0411		
CP1b	0412		
CP1c	0413		
CP2a	0421		
CP2b	0422		
CP3	0043		
S	0005		
I1	0061		
I2	0062		
I1F	0616		

TABLE 7

TYPICAL SNOW CRYSTAL REPLICA DATA,
 HAO, CLIMAX, COLORADO
 5 January 1967

Site	Date	Time (MST)	Surface Temp. (-° C)	Film Rate (in/min)	Slit Width (in)	Crystal Form	Crystal Size		Formation Temp. (-° C)	No. Crystals Area	Area (mm ²)						
							Length (μ)	Width (μ)									
001	01 05 67	2110	09	3.33	1.00	0311	0210	0250	14	001	450						
		↓				0061	0010		25	001							
		2112				0311	0110		14	001							
		↓				0213	0110		20	001							
		2124				0061	0100		25	001							
		↓				0311	0130		14	001							
		↓				0210				004							
		↓				0290				001							
		↓				0212	0210		0090	20		001					
		↓				0213	0170		0040			001					
		↓					0190		0040			001					
		↓					0150		0090			001					
		↓					0210		0090			002					
		↓					0210		0110			002					
		↓					0210		0150			001					
		↓					0222		0450	0130		001					
		↓					0043		0250			005					
		↓					0610		0170			001					
		↓					0061		0110			048					
		(2125 to 2359 and a portion of 2400 deleted)															
							2400		12	3.15		0.50	0213	0250	0030	20	002
							↓							0250	0240		001
							↓							0280	0030		001
							↓							0310	0030		001
							↓							0330	0050		001
							↓						0222	0170	0140		001
							↓						0430	0150		25	001
							↓							0170			001
							↓							0190			002
							↓							0310			001
		↓					0610			001							
		↓				0043	0250			054							
		↓				0061	0230			001							
001	01 06 67	0000	Etc.														

separate data card: time (4 digits, columns 1-4), surface temperature (2 digits, columns 5-6), film rate (4 digits, columns 7-10), slit width (4 digits, columns 11-14), crystal form (4 digits, columns 15-18, [from Figure 17 and Tables 5 and 6]), crystal length (4 digits, columns 19-22), crystal width (4 digits, columns 23-26, [for crystal types 0111, 0112, 0211, 0212, 0213, 0221, 0222 only]), formation temperature (2 digits, columns 27-28, [from Figure 2]), number of crystals per area (3 digits, columns 29-31), area of grid (3 digits, columns 32-34). Additional identification cards are placed within the snow crystal data cards whenever the date changes or the snowfall period ends in a snowstorm. The card preceding an inserted identification card must have an * in column 80. Snow crystal observations can be made at any time interval on the film, however, an observation must be made at each hour during the snowfall period. Also, when the date changes, the 2400-hour data cards must be duplicated with the time changed to 0000-hour, and the duplicated cards placed on the opposite side of the identification card. These hourly observations, plus duplicated cards permit continuity between the snow crystal plots produced by the computer in Figures 9, 11, and 12.

Snow Crystal Concentration Program

The initial snow crystal concentration computation scheme is described by Hindman and Rinker (1967). The system uses

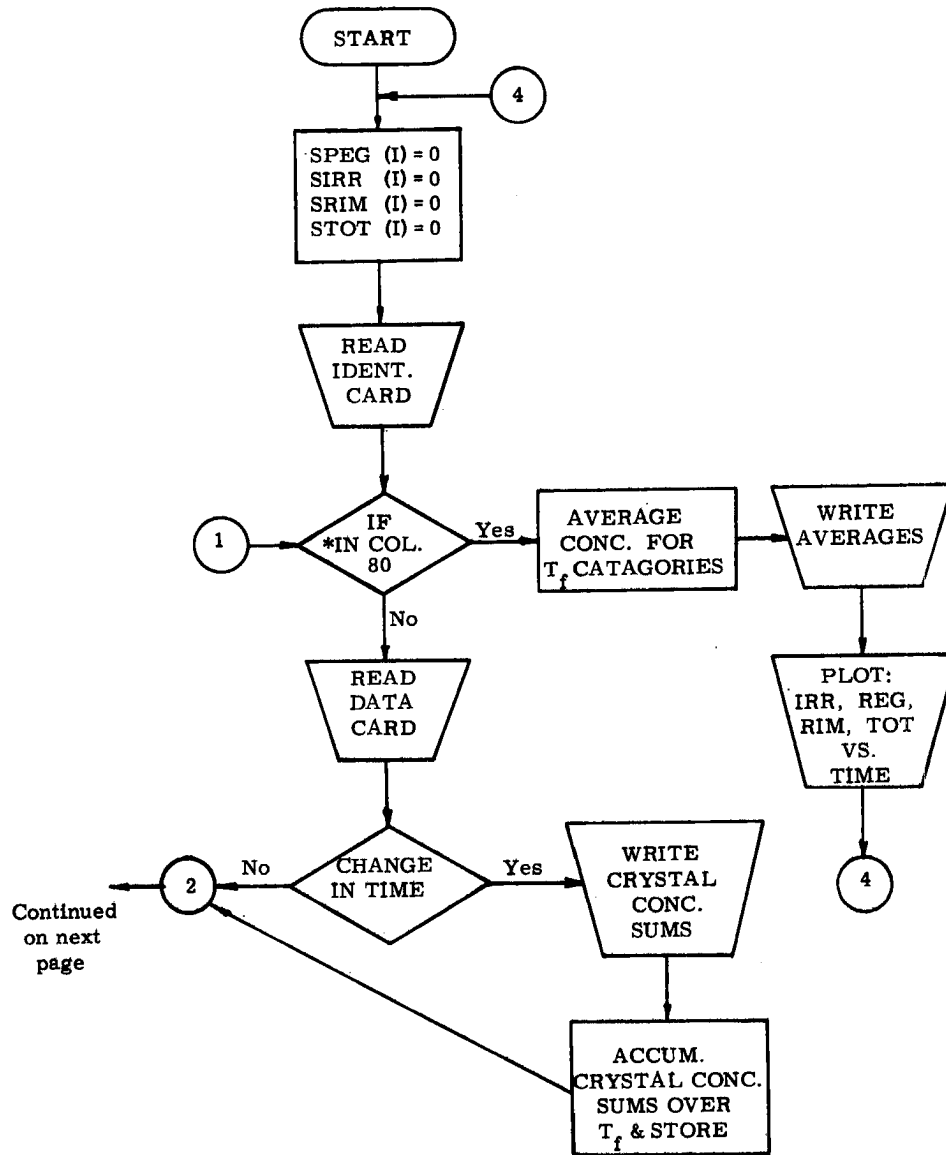
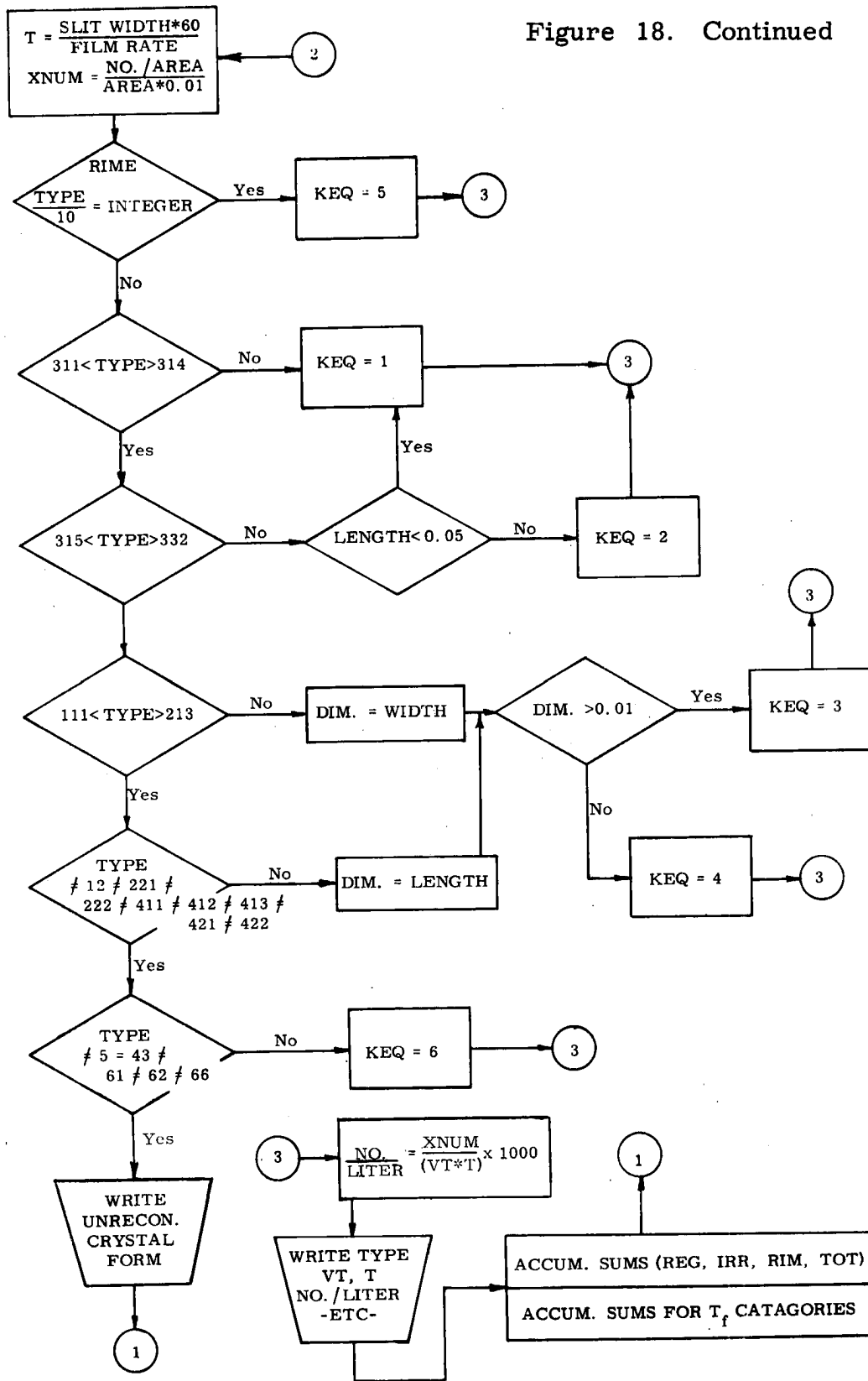


Figure 18. Snow crystal concentration computer program flow-chart

Figure 18. Continued



```

PROGRAM SNOTY
DIMENSION IPBTRN(4)
DIMENSION ILAR1(2)
DIMENSION SREG(1500),SIRR(1500),STOT(1500),SRIM(1500),ITIM(1500)
DIMENSION ILAR(2),TIME(1500)
DIMENSION IV(5)
INTFGER P1
CORR = 5./3.
IPBTRN(1)=12528 $ IPBTRN(2)=16668 $ IPBTRN(3)=11118 $ IPBTRN(4)=17
FT14 = 0 $ FT20 = 0 $ FT26 = 0
1778
C   KHEd IS SWITCH FOR CONTROL OF PLOTTING
    KHEd=1
C   IF IKH IS AN * END OF THIS SET OF DATA
C   IF IKH IS AN A THE NEXT CARD MUST BE A VARIABLE FORMAT CARD
    IKH = 1HA
10 GO TO (14,20)KHEd
14 IF (IKH.EQ.1H*)GO TO 26
15 DO 16 J=1,1500
    SREG(J)=0.0
    SIRR(J)=0.0
    STOT(J)=0.0
    SRIM(J)=0.0
16 ITIM(J)=0
C   READ SITE AND DATE CARD
    READ(5,17)ISITE,IDAT
17 FORMAT(I3,I6)
    WRITE(6,18)ISITE,IDAT
C   WRITE SITE AND DATE CARD
18 FORMAT(*1SITE *I3,* DATE *I6)
    J=1
    I=2
500 FORMAT (I2X,5A10)
20 IF (IKH.NE.1HA) GO TO 21
C   READ VARIABLE FORMAT CARD
    READ(5,500)(IV(I),I=1,5)
C   READ DATA CARD
21 READ(5,IV)ITIM(I),ISFT,FIL,SLW,P1,XLEN,WID,IFOT,INUM,AREA,IKH
C   CHECK FOR CHANGE IN TIME
    IF(KHEd.EQ.1) ITIM(1)=ITIM(2)
    IF(ITIM(I).EQ.ITIM(I-1))GO TO 27
C   COMPUTE SUM OF TOTAL NUMBER OF CRYSTALS PER LITER
26 STOT(I)=SIRR(I)+SREG(I)+SRIM(I)
    WRITE(6,171) ITIM(I-1)
171 FORMAT(*0 TIME *I4)
C   WRITE SUMS OF REGULAR,IRREGULAR,RIME AND TOTAL
    WRITE(6,170)SREG(I),SIRR(I),SRIM(I),STOT(I)
170 FORMAT(*0 SUM OF REGULAR CRYSTALS PER LITER*F20.10/5X,*SUM OF
1IRREGULAR CRYSTALS PER LITER*F20.10/10X,*SUM OF RIME CRYSTALS PER
2 LITER*F20.10/10X,*SUM OF TOTAL CRYSTALS PER LITER*F20.10)
C   COMPUTE OVERALL CONCENTRATIONS FOR TEMPERATURES OF -14,-20,-26
    FT14 = FT14 + F14
    FT20 = FT20 + F20
    FT26 = FT26 + F26
C   WRITE CONCENTRATIONS FOR SPECIFIC TIME
    WRITE (6,501)F14,F20,F26
C   WRITE AVERAGES OF CONCENTRATIONS AT -14,-20,-26
501 FORMAT(*0 CONCENTRATION OF CRYSTALS*/10X,*AT FORMATION TEMPERATURE
1 GREATER THAN OR EQUAL TO -14*F20.5/10X,*AT FORMATION TEMPERATURE
2 GREATER THAN OR EQUAL TO -20*F20.5/10X,*AT FORMATION TEMPERATURE
3 GREATER THAN OR EQUAL TO -26*F20.5)
    F14 = 0 $ F20 = 0 $ F26 = 0

```

Figure 19. Snow crystal concentration computer program

Figure 19. Continued

```

405 K1 = K1 + 1
    IF (TIME(K1).GT.AXIS2.OR.K1.GT.J) GO TO 415
    CALL VECTOR (TIME(K1),STOT(K1+1))
    GO TO 405
415 IPATRN = 1252B
    CALL DASHLN (IPATRN)
    K1=K1-1
C   PLOT NUMBER OF IRREGULAR CRYSTALS
    CALL FRSTPT (TIME(K2),SIRR(K2+1))
406 K2 = K2 + 1
    IF (TIME(K2).GT.AXIS2.OR.K2.GT.J) GO TO 416
    CALL VECTOR (TIME(K2),SIRR(K2+1))
    GO TO 406
416 IPATRN = 1666B
    CALL DASHLN (IPATRN)
    K2=K2-1
C   PLOT NUMBER OF REGULAR CRYSTALS
    CALL FRSTPT (TIME(K3),SREG(K3+1))
407 K3 = K3 + 1
    IF (TIME(K3).GT.AXIS2.OR.K3.GT.J) GO TO 417
    CALL VECTOR (TIME(K3),SREG(K3+1))
    GO TO 407
417 IPATRN = 1111B
    CALL DASHLN (IPATRN)
    K3=K3-1
C   PLOT NUMBER OF RIME CRYSTALS
    CALL FRSTPT (TIME(K4),SRIM(K4+1))
408 K4 = K4 + 1
    IF (TIME(K4).GT.AXIS2.OR.K4.GT.J) GO TO 418
    CALL VECTOR (TIME(K4),SRIM(K4+1))
    GO TO 408
418 IPATRN = 1777B
    CALL DASHLN (IPATRN)
    CALL FRAME
    IF (K4.GE.I) GO TO 15
    K4=K4-1
601 AXIS1=AXIS1+200.0
    AXIS2=AXIS2+200.0
    IF (TIME(K1+1).GE.AXIS2) GO TO 601
    IF (TIME(K1).EQ.AXIS1) GO TO 430
    K1 = K1 + 1
    K2 = K2 + 1
    K3 = K3 + 1
    K4 = K4 + 1
    GO TO 430
C   END OF PLOTTING ROUTINE
C   COMPUTE TERMINAL VELOCITY AND NUMBER CRYSTALS OF FOR EACH CARD
401 ITIM(I+1) = ITIM(I)
400 J=J+1
    I=I+1
27  KFO = 0
    KHED=2
    IF (IKH.EQ.1H*) KHED=1
    IF (P1.EQ.0) GO TO 300
    VT=0
    ISFT=-ISFT
    IFOT=-IFOT
    T=SLW*60./FIL
    XLEN=.0001*XLEN
    WID=.0001*WID
    XNUM=INUM/(AREA*.01)
    SXNUM=XNUM/T
    P11=XMODF(P1,10)

```

APPENDIX B

Terminal Velocities of Snow Crystals

The terminal velocities of snow crystals must be known to determine the volume of air from which they settle. This volume is given by:

$$V = V_t t A$$

where $V_t(\text{cm sec}^{-1})$ is the terminal velocity of a specific crystal type, and $t(\text{sec})$ is the exposure time of an area on the film, $A(\text{cm}^2)$. Todd (1964) made an extensive compilation of the terminal velocities of snow crystals from the literature in Figure 20. The terminal velocity equations (KEQ) for the snow crystal concentration computer program in Figure 19 are derived from Figure 20.

Terminal velocities for rimed and plane dendritic snow crystals were among those measured by Nakaya (1954). First, the author fit a power curve to Nakaya's data and derived an expression for the terminal velocities of rimed crystals:

$$V_t = 125.7 d^{0.084} \quad (\text{KEQ} = 5)$$

where V_t is the terminal velocity (cm sec^{-1}), and d is the diameter of the crystal (cm). This diameter is defined as the largest

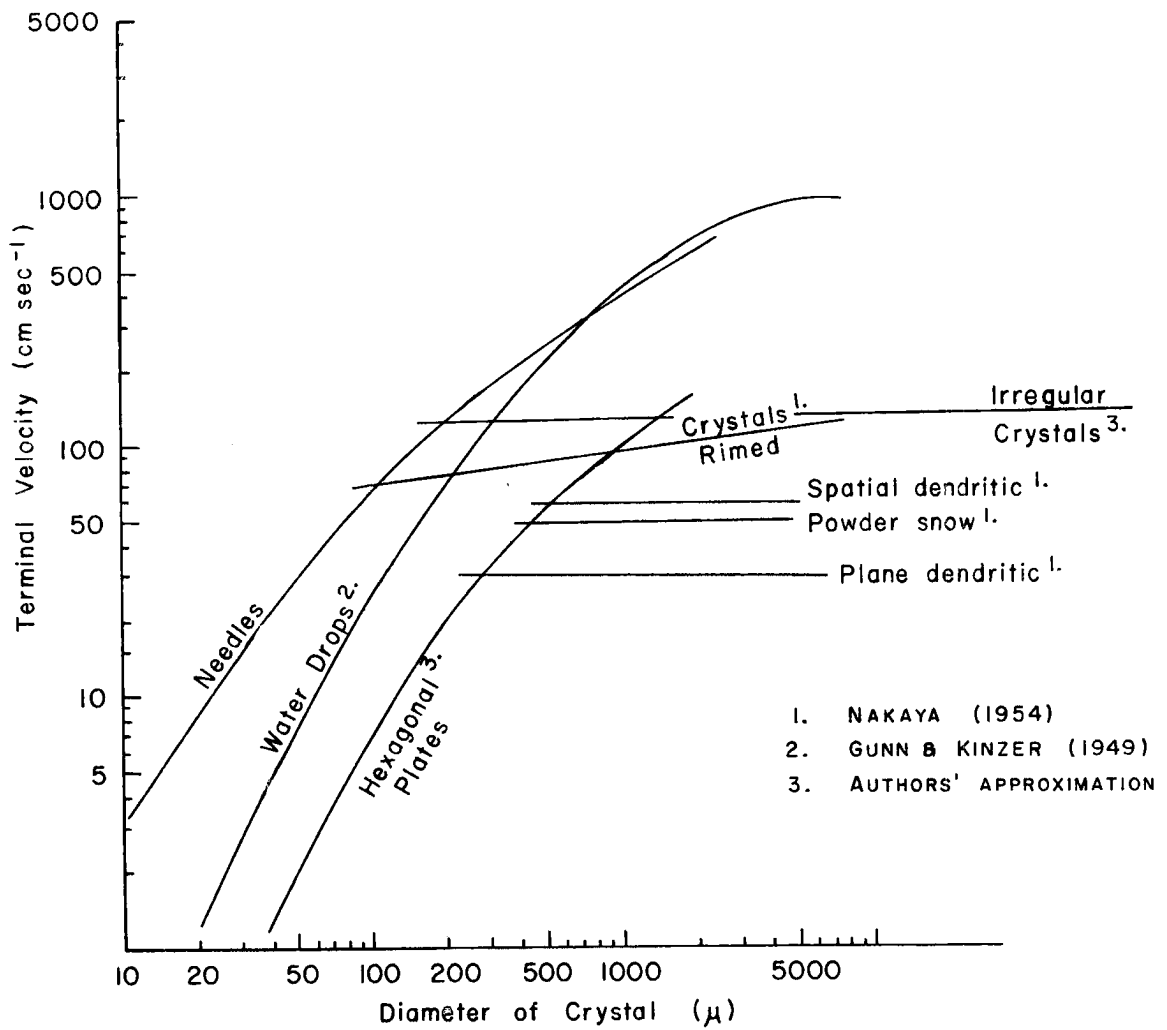


Figure 20. Terminal velocities of various snow crystals [from Todd (1964)]

dimension in any direction. The equation is used for any crystal form in Table 6 ending in zero. It is assumed valid for any rimmed crystal size.

Nakaya found that plane dendritic crystals fall at a constant 30 cm sec^{-1} . The terminal velocity equation for plane dendritic crystals is therefore,

$$V_t = 30 (\text{cm sec}^{-1}) \quad (\text{KEQ} = 2)$$

The author assumes that this equation is valid for crystal types between 0321 and 0332 in Table 6 with diameters greater than or equal to 0.050 cm. The plane dendritic crystal diameter is defined as the longest length from point to point. Below 0.050 cm, the equation for hexagonal plates is used.

The hexagonal plate equation was generated by a "least squares fit" computer program which fits a cubic equation to the hexagonal plate curve in Figure 20. The hexagonal plate equation (KEQ = 1) and solutions are listed in Table 8. This equation is valid for all sizes of crystal types in Table 6 between 0311 and 0314, and for crystal types between 0321 and 0332 with diameters less than 0.050 cm.

The "least squares fit" computer program was used to generate the terminal velocity equations for the needle crystal curve in Figure 20. Two equations were derived. The needle

TABLE 8

HEXAGONAL PLATE TERMINAL VELOCITY
EQUATION AND SOLUTIONS

Hexagonal Equation	
$V_t = -2.78 + 1927.35 D - 32073.70 D^2 + 173775.17 D^3$	
Hexagonal Solutions	
Diameter (cm)	Terminal Velocity (cm sec ⁻¹)
0.0001	-2.59
0.0011	-0.70
0.0031	2.88
0.0061	7.81
0.0091	12.23
0.0121	16.41
0.0181	22.62
0.0211	25.23
0.0241	27.46
0.0271	29.35
0.0301	30.90
0.0331	32.17
0.0391	33.92
0.0421	34.47
0.0451	34.84
0.0481	35.05
0.0511	35.14
0.0541	35.12
0.0601	34.92
0.0631	34.78
0.0661	34.66
0.0691	34.58
0.0721	34.57
0.0751	34.66
0.0781	34.88
0.0841	35.82
0.0871	36.59
0.0901	37.60
0.0931	38.87
0.0991	42.35

equation (KEQ = 3) in Table 9 is valid for crystals with dimensions less than or equal to 0.010 cm. The needle equation (KEQ = 4) in Table 10 is valid for crystals with dimensions greater than or equal to 0.011 cm. The needle equation is assumed valid for columns since they have similar shapes. Needle and column dimensions are defined as both their length and width. The length dimension is used for crystal types 0012 and 0411 to 0422. The width dimension is used for crystal types 0111, 0112, and 0211 to 0222.

Rinker (private communication) has measured terminal velocities of snow crystals using Nakaya's (1954) technique. The author approximated the terminal velocity of irregular crystals from this data to be 120 cm sec^{-1} . For simplicity, since the dimensions are irregular, the terminal velocity is assumed constant with size. The terminal velocity equation is therefore,

$$V_t = 120 (\text{cm sec}^{-1}) \quad (\text{KEQ} = 6)$$

This equation is valid for crystal types 0043, 0005, 0061, 0062, 0616 in Table 6. The average size for the total number of irregular crystals of each type on the film are recorded in Table 7 since KEQ = 6 is not a function of size.

TABLE 9

NEEDLE TERMINAL VELOCITY EQUATION AND SOLUTIONS
(Crystal Dimension ≤ 0.010 cm)

Needle Equation	
$V_t = -3.09 + 5268.58 D + 351293.25 D^2 - 20028419.31 D^3$	
Needle Solutions	
Dimension (cm)	Terminal Velocity (cm sec ⁻¹)
0.001	2.50
0.002	8.69
0.003	15.33
0.004	22.32
0.005	29.53
0.006	36.84
0.007	44.13
0.008	51.28
0.009	58.17
0.010	64.69

TABLE 10

NEEDLE TERMINAL VELOCITY EQUATION AND SOLUTIONS
(Crystal Dimension ≥ 0.011 cm)

Needle Equation	
$V_t = -6.21 + 7744.39 D - 65408.58 D^2 + 260855.13 D^3$	
Needle Solutions	
Dimension (cm)	Terminal Velocity (cm sec ⁻¹)
0.010	64.94
0.012	77.74
0.015	96.11
0.018	113.51
0.021	129.98
0.024	145.57
0.030	174.29
0.033	187.49
0.036	199.98
0.039	211.80
0.042	222.99
0.045	233.59
0.051	253.22
0.054	262.32
0.057	277.00
0.060	279.32
0.063	287.29
0.066	294.98
0.072	309.66
0.075	316.73
0.078	323.68
0.081	330.56
0.084	337.39
0.087	344.24
0.093	358.11
0.096	365.22
0.099	372.51
0.102	380.02
0.105	387.78
0.108	395.85